BEILSTEIN JOURNAL OF ORGANIC CHEMISTRY

Photocatalysis and photochemistry in organic synthesis

Edited by Timothy Noël and Bartholomäus (Bart) Pieber

Imprint

Beilstein Journal of Organic Chemistry
www.bjoc.org
ISSN 1860-5397
Email: journals-support@beilstein-institut.de

The *Beilstein Journal of Organic Chemistry* is published by the Beilstein-Institut zur Förderung der Chemischen Wissenschaften.

Beilstein-Institut zur Förderung der Chemischen Wissenschaften
Trakehner Straße 7–9
60487 Frankfurt am Main
Germany
www.beilstein-institut.de

BEILSTEIN JOURNAL OF ORGANIC CHEMISTRY

Negishi-coupling-enabled synthesis of α-heteroaryl-α-amino acid building blocks for DNA-encoded chemical library applications

Matteo Gasparetto, Balázs Fődi and Gellért Sipos*

Full Research Paper

Open Access

Address:
X-Chem Zrt., Záhony u. 7, DA Building, Graphisoft Park, Budapest, 1031, Hungary

Email:
Gellért Sipos* - gellert.sipos@x-chemrx.com

* Corresponding author

Keywords:
amino acids; DEL; flow chemistry; Negishi; on-DNA chemistry

Beilstein J. Org. Chem. **2024,** *20,* 1922–1932.
https://doi.org/10.3762/bjoc.20.168

Received: 30 May 2024
Accepted: 26 July 2024
Published: 08 August 2024

This article is part of the thematic issue "Photocatalysis and photochemistry in organic synthesis".

Guest Editor: T. Noël

Abstract

Amino acids are vital motifs in the domain of biochemistry, serving as the foundational unit for peptides and proteins, while also holding a crucial function in many biological processes. Due to their bifunctional character, they have been also used for combinatorial chemistry purposes, such as the preparation of DNA-encoded chemical libraries. We developed a practical synthesis for α-heteroaryl-α-amino acids starting from an array of small heteroaromatic halides. The reaction sequence utilizes a photochemically enhanced Negishi cross-coupling as a key step, followed by oximation and reduction. The prepared amino esters were validated for on-DNA reactivity via a reverse amidation–hydrolysis–reverse amidation protocol.

Introduction

DNA-encoded chemical library (DEL) technology is a powerful tool for hit identification [1,2]. DELs are chemically synthesized libraries in which every member is covalently attached to a unique DNA sequence serving as a molecular "barcode" [3]. The success of this technology ultimately relies on the quality and diversity of the libraries. DEL synthesis must employ DNA-compatible reactions; hence it operates under a limited set of conditions [4,5]. DELs are typically produced via split-and-pool combinatorial chemistry methods. Using bifunctional building blocks (BBs) can quickly increase the diversity of these molecular libraries [6]. Hence, DEL practitioners constantly seek access to novel building blocks [7].

Amino acids (AAs) are vital motifs in the domain of biochemistry, serving as the foundational unit for peptides and proteins, while also holding a crucial function in many biological processes [8]. Non-canonical amino acids (NCAs) are widely used in medicinal chemistry [9]. Not surprisingly, they also find broad use as bifunctional building blocks (BBs) for DELs. In an early example, an 800-million-members DEL utilized Fmoc-amino acids as primary diversity elements [10].

The pursuit of achieving the efficient synthesis of α-amino acids has been an ongoing challenge since 1850, marked by the initial report of the Strecker condensation [11]. The Strecker synthesis

and the related Bucherer–Bergs hydantoin formation remains the most employed approach for producing this family of substrates [12]. Despite its effectiveness, this approach requires hazardous cyanides and harsh conditions for the subsequent hydrolysis of the nitrile or the hydantoin. Additionally, it carries significant limitations in its scope, reducing its overall applicability.

A different approach for the synthesis of α-amino acids involves the formation of dehydroamino acids and subsequent hydrogenation [13,14]. More recently, there have been reports of techniques that utilize phase transfer catalysts (PTCs) to alkylate glycine derivatives [15,16]. A range of less widely applicable strategies have been developed as well [17-22].

The above-mentioned methods focus on the synthesis of α-alkyl-amino acids. Moving to α-aryl-amino acids, the Clayden group published an excellent asymmetric α-arylation method to access quaternary amino acids with high enantiomeric purity [23]. The synthesis of formally glycine-derived tertiary α-aryl-amino acids is much less developed. The most common strategy for obtaining these substrates is by lithiation of an aromatic ring followed by coupling with a glycine derivative (Scheme 1a). For example, this approach was applied to the synthesis of *N*-substituted pyrazoles and poly-substituted isothiazoles [24,25]. Glycine derivatives can be reacted with indoles using copper catalysis or metallophotoredox catalysis [26]. Le et al. reported the use of the same approach for imidazo[1,2-*a*]pyridines [27,28]. However, the selectivity of these photoredox reactions is driven by the structural properties of the heteroaromatic ring. During the preparation of this article, the Meggers group published an outstanding enantioselective iron-catalyzed α-amination pathway (Scheme 1b) [29]. The method is widely applicable to a broad range of substrates, however, it utilizes a catalyst that is not commercially available and small heteroaromatic rings are underrepresented in the scope.

Recognizing the importance of small heteroaromatic rings and the amino acid motif in medicinal chemistry [30-33], and aiming to expand our in-house DEL BB collection, we sought to develop a synthetic route capable of providing a broad range of α-heteroaryl-α-amino acids in a cost-effective manner (Scheme 1c).

Herein, we describe the synthesis and on-DNA validation of non-canonical α-heteroaryl-α-amino acids. We envisioned that α-heteroaryl acetates accessed through Negishi coupling can be used as key intermediates towards NCAs (Scheme 1c). Indeed, oximation of these motifs followed by reduction gave access to the desired NCAs.

Results and Discussion

Negishi cross-coupling step

The Negishi reaction provides convenient access to compounds featuring C(sp^2)–C(sp^3) bonds. However, the general view is

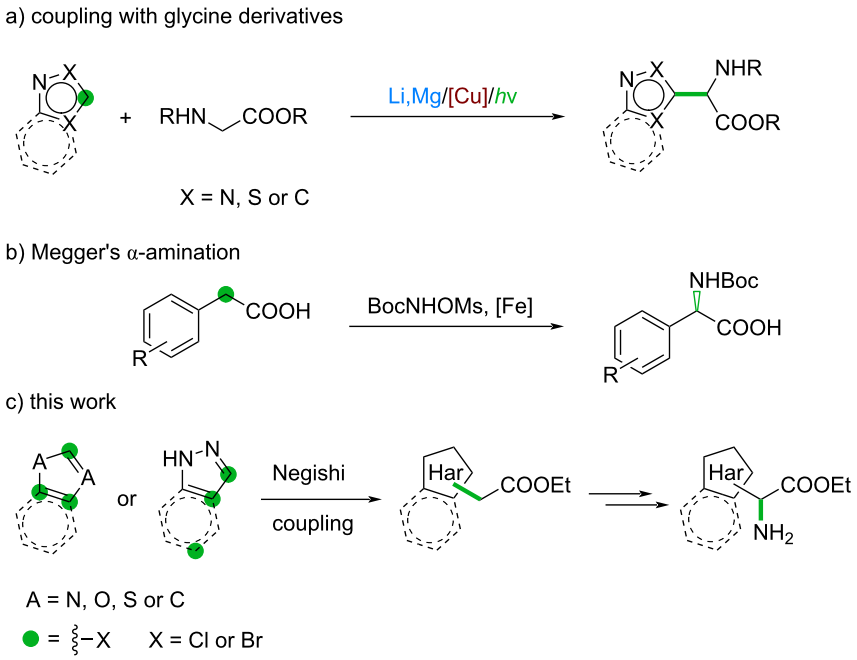

Scheme 1: Known and improved synthetic strategies to access α-(hetero)aryl-amino acids.

that this transformation is less reliable than its orthogonal counterpart, the Suzuki reaction. Recent years have seen significant developments in Negishi reaction methodologies [34-39]. In particular, Alcazar et al. developed continuous flow protocols for both the generation of alkylzinc halides and for the subsequent Negishi cross-coupling reaction [40-44]. We successfully adapted Alcazar's protocols for the synthesis of otherwise challenging heteroaryl–alkyl connections (see Table S1 in Supporting Information File 1). We decided to explore the potential of this methodology for the formation of α-heteroarylacetates. In particular, we were curious to see whether this methodology translates well for five-membered heteroarene substrates (e.g., thiazoles, pyrazoles, imidazoles) which are usually underrepresented in the peer-reviewed literature in comparison to phenyl groups or their six-membered counterparts (e.g., pyridines, pyrimidines) [42]. Furthermore, the increasing importance of small heteroaromatic rings containing nitrogen, sulfur and/or oxygen in medicinal chemistry is well depicted by the list of recently approved drugs by the FDA [31]. Fezolinetant (an NK3 receptor antagonist) and quizartinib (FLT3 inhibitor) are just a couple of examples among the drugs reaching the market in the last year.

As shown in Scheme 2, ethyl (bromozinc)acetate (**1a**) was synthesized in flow by pumping a solution of ethyl 2-bromoacetate through a pre-activated zinc column (see page 11 in Supporting Information File 1) [44]. The Reformatsky reagent could be obtained in yields varying from 70 to 90% depending on the activation state of the column. The yield of the reaction was determined by titration with iodine (see page 11 Supporting Information File 1), affording final concentrations between 0.35 to 0.45 M in THF. The solution can be stored in the fridge under argon for one week before being used in the Negishi reaction. With concentrations above 0.4 M we observed crystallization of ethyl (bromozinc)acetate at the bottom of the vial after a few hours of storage in the fridge. The solid can be easily re-dissolved by gentle heating, and without affecting the product concentration and integrity.

After a brief screening, $Pd(dba)_2$ and X-Phos (in a 1:2 ratio) were selected as the catalyst system for the Negishi reaction (Supporting Information File 1). Preliminary experiments were carried out with and without blue light irradiation in the PhotoCube^{TM} photoreactor [45]. These experiments revealed that while the conversion of imidazoles and pyrazoles benefits from irradiation, thiazoles seem to be largely unaffected by the presence of light (see pages 5 and 6 in Supporting Information File 1). In the case of indazoles, increased reaction rates were observed in the presence of light, but the overall yield was the same for the dark and irradiated experiments. Although these reactions are typically complete within 4 h in the dark, irradiation with blue light halves the reaction time for many compounds. Overall, these observations are in line with those of Alcazar et al. [43]. In their work, the authors demonstrated the formation of a complex between palladium and the organozinc reagent which is absorbing in the blue region. This complex then accelerates the oxidative addition of the aryl halide to the metal, which is usually the rate-limiting step for palladium-catalyzed cross-couplings. Based on these results we decided to perform all Negishi reactions under blue light irradiation.

With the optimized conditions in hand, we proceeded with the investigation of the heteroaryl halide scope in batch (Scheme 3). Thiazoles proved to be challenging substrates typically affording the desired products in moderate yields (**2b**–**h**). While 2-chlorothiazole led to the production of **2b** in 44% yield, 2-bromo-5-chlorothiazole only afforded 21% yield (**2d**). Gratifyingly, the reaction selectively proceeded in position 2 of the ring. Position 4 seems to be inert to the Negishi coupling conditions as illustrated by substrates **2c** and **2g**. Somewhat surprisingly, LCMS analysis indicated that **1g** did not go through oxidative addition and remained unreacted. Formation of **2h** did not occur, however, we observed the formation of unidentified side products. Interestingly, the presence of a free carboxylic group is well tolerated (**2f**). Benzothiazole **1i** proved to be an excellent substrate for this reaction, leading to the desired acetate **2i** in high yield. A similar result was obtained for the furanyl derivative **2j**. Pyrazoles were the only substrate class which clearly benefited from light irradiation (**2k**–**o**), displaying not just a shorter reaction time but also higher yields. Even unprotected pyrazoles (**2k**, **2m**, **2n**) performed well, showing that *N*-protection is not mandatory for this transformation.

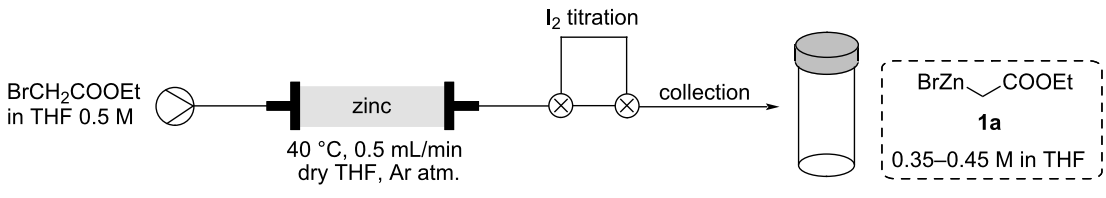

Scheme 2: Reformatsky reagent production.

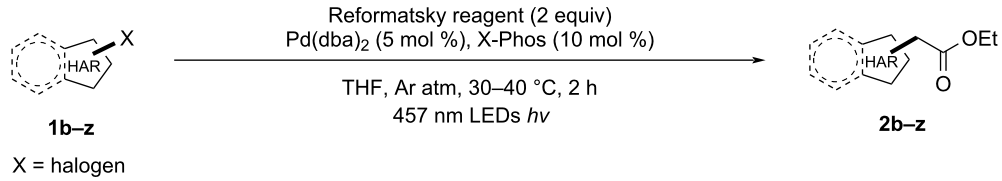

1b–z

X = halogen

2b–z

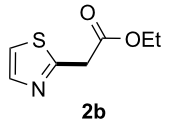

2b

44% (X = Cl)

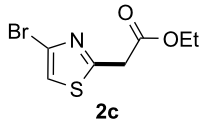

2c

62% (X = Br)

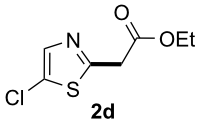

2d

21% (X = Br)

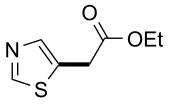

2e

50% (X = Br)

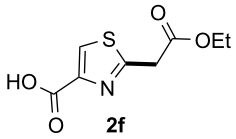

2f

61% (X = Br)

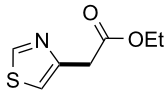

2g

– (X = Br)

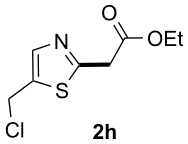

2h

– (X = Cl)

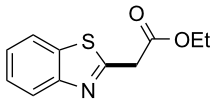

2i

87% (X = Br)

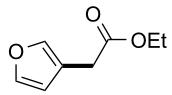

2j

87% (X = Br)

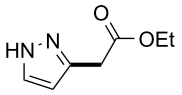

2k

73% (X = Br)
not irradiated: 45%*

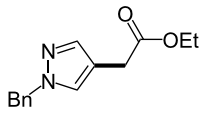

2l

80% (X = Br)
not irradiated: 58%*

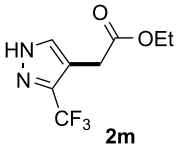

2m

95% (X = Br)
not irradiated: 66%*

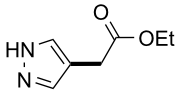

2n

48% (X = Br)
not irradiated: 26%*

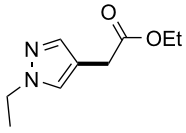

2o

87% (X = Br)

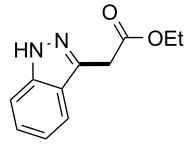

2p

39% (X = Cl)

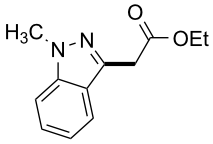

2q

48% (X = Br)

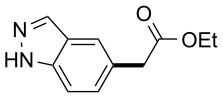

2r

82% (X = Br)

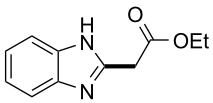

2s

– (X = Br)

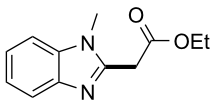

2t

77% (X = Br)

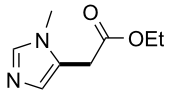

2u

92% (X = Br)

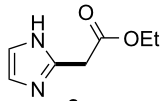

2v

– (X = Br)

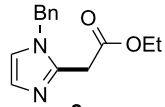

2z

– (X = Br)

Scheme 3: Scope of ethyl heteroarylacetates. Isolated yields are given. *Dark reactions were carried out for 4 h.

3-Bromo- and 3-chloroindazoles offered moderate yields (39% and 48% for **2p** and **2q**, respectively), while 5-substituted **2r** was isolated with 82% yield. In contrast to pyrazoles and indazoles, benzimidazoles and imidazoles required the protection of the aromatic NH group (**2s** vs **2t**; **2v** vs **2u**). Reactions with unprotected imidazoles **1s** and **1v** led to immediate formation of a precipitate upon addition of the Reformatsky reagent. Surprisingly, **1z** did not afford the expected product (**2z**).

The synthesis of the Reformatsky reagent can be combined with the Negishi cross-coupling step in a continuous flow manner [41-43]. Continuous flow chemistry offers superior control over reaction parameters compared to traditional batch methods. This approach leads to reproducible reactions, improved safety features, and it can facilitate high-throughput screening and rapid optimization [46,47]. Homogenous heating and mixing in flow reactors can lead to higher reaction rates and yields. In terms of photochemistry, continuous flow setups provide enhanced light irradiation as well [48,49]. These advantages make flow chemistry a powerful tool for chemical synthesis and industrial applications [50,51].

To assess the advantage of moving from batch to flow, the production of compounds **2b** and **2i** was carried out with the telescoped approach. Despite the difference in the yield being minimal, the rate of the transformation showed a significant improvement under continuous flow conditions, leading to reaction completion within 30 minutes (Scheme 4).

Oxime formation

Once the ethyl heteroarylacetates scope was completed we turned our attention to the incorporation of the amino group. There are precedents for α-aminations, but we were not able to find a method suitable for our needs [52,53]. Benzylic bromination followed by nucleophilic substitution offers a general approach for the introduction of the nitrogen atom [54-56]. Consequently, the continuous flow Wohl–Ziegler bromination of **2b** was attempted [57]. Even though we could observe excellent LCMS-conversion for the mono-brominated compound, we encountered several problems related to the stability of the product (see Supporting Information File 1).

To circumvent these issues, we came across the possibility of inserting an oximino group into the benzylic position which can then be converted into an amino group by reduction. We reasoned that increasing the sp^2 fraction and the rigidity of the whole structure will lead to increased stability of these derivatives. The first exploratory attempts demonstrated the easy preparation and the high bench stability of the oxime derivatives, therefore we opted to proceed using this route. In this study, we explored three distinct approaches commonly employed for the introduction of the oximino group into a molecule. The first approach is based on the generation of the nitrosonium ion from sodium nitrite under acidic conditions (Scheme 5, top) [58,59]. Additionally, another very common method involves the employment of a strong base, typically sodium ethoxide or methoxide, in combination with an alkyl nitrite to promote the incorporation of the oximino group (Scheme 5, middle) [60,61]. Furthermore, a widely adopted strategy involves the conversion of a carbonyl group to an oxime through condensation with hydroxylamine (Scheme 5, bottom) [62-64].

In order to develop a synthetic approach applicable to several different substrates, we decided to screen the three methods on one example from each type of heteroaryl halides. According to

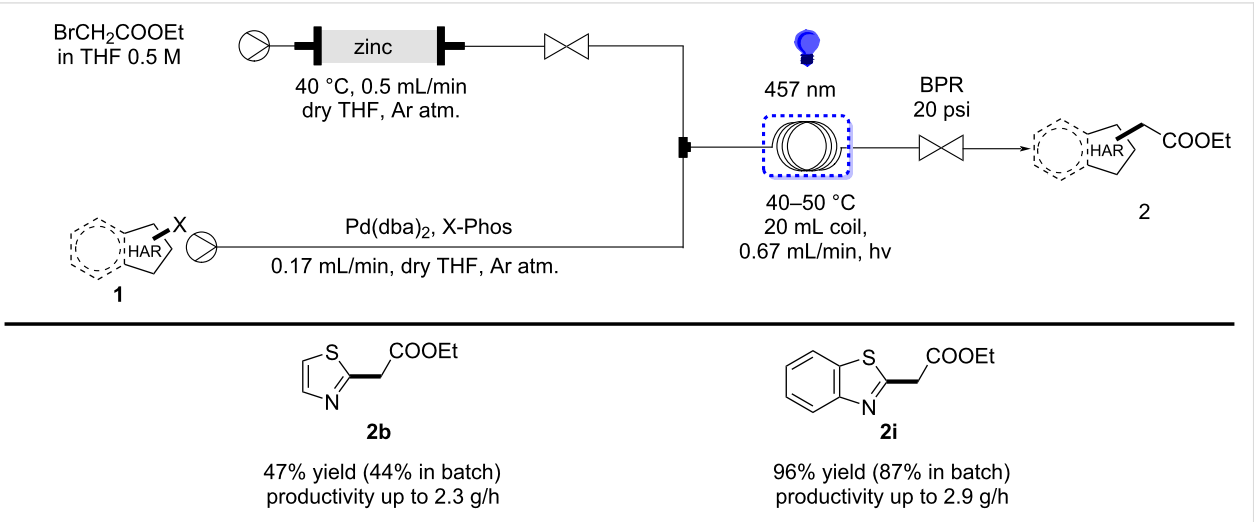

Scheme 4: Telescoped flow synthesis of heteroarylacetates.

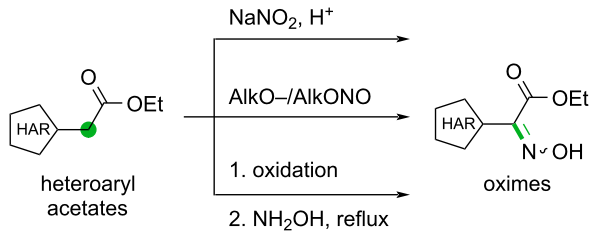

Scheme 5: Potential routes for the preparation of oximes.

our experimental results, thiazole **2b**, benzothiazole **2i** and benzimidazole **2t** react very well with sodium nitrite in an acidic environment (Scheme 6, red section). Among the various subclasses of compounds, pyrazole **2l** exhibited a high reactivity using *t*-BuONO and EtONa in ethanol (Scheme 6, red section). On the other hand, no reaction was observed with indazoles and furans using the first two conditions, requiring the formation of the ketoesters **4j** and **4r** first, followed by the functional group interconversion (FGI) with $NH_2OH{\cdot}HCl$ (Scheme 6, blue and green sections).

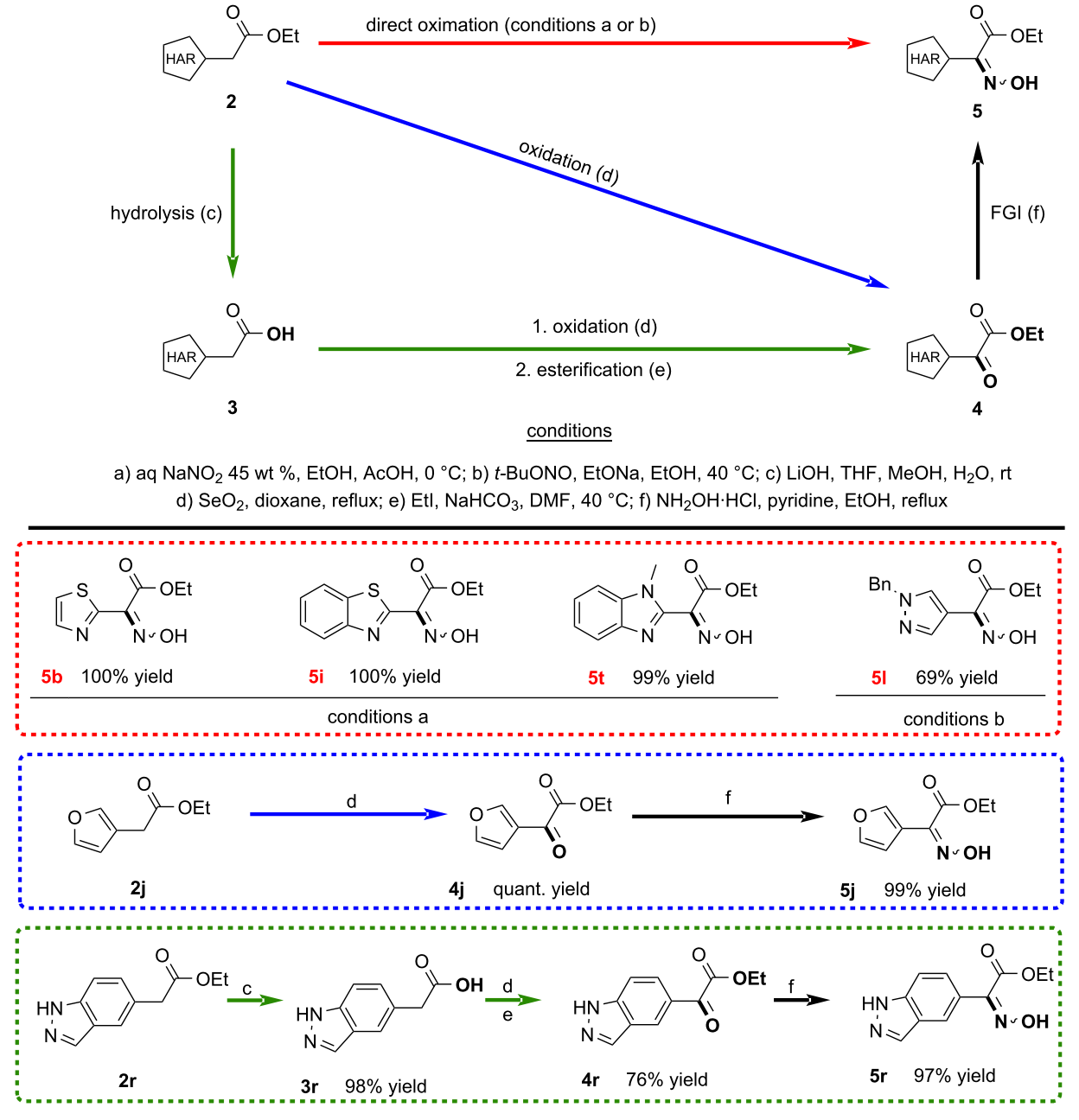

Scheme 6: Oxime group insertion step.

The Riley oxidation of the furanyl derivative **2j** proceeded smoothly yielding **4j** in quantitative yield. However, obtaining compound **4r** presented some challenges due to the resistance of ester **2r** towards conventional oxidation methods (see Table S5 in Supporting Information File 1). Consequently, a multistep process involving ester hydrolysis and subsequent re-esterification was necessary to achieve the desired ketoester.

Reduction of the oximes

Oximes are commonly reduced to the corresponding amines using either palladium on activated carbon and hydrogen gas [65-68], or with zinc and a Brønsted acid as source of hydrogen [68,69]. Both methods were tested and after a brief optimization process, zinc dust and HCl in a mixture of EtOH/dioxane proved to be the best conditions in order to maximize the yield and limit the amino ester instability issues (see Table S6 in Supporting Information File 1). By slightly adjusting the reaction time and the temperature, all oxime derivatives underwent reduction to yield the corresponding amine. The amino esters were effectively safeguarded against degradation through the immediate formation of the HCl salt or by Boc-protection. This procedure allowed us to obtain all the protected amino acids in a yield that varies from 56 to 74% (Scheme 7).

Gram scale experiment

With the optimized synthetic route, we were able to reach the final targets in good to excellent overall yields (from 25% to 64%, see Scheme 7). To test the robustness of our approach, the synthesis of compound **6i** was carried out on gram scale starting from 2.1 g of 2-bromobenzothiazole (**1i**). The gram scale production showed comparable results to those obtained in the small-scale procedure, leading to the formation of 1.8 g (67% overall yield) of the final product **6i** (Scheme 7, bottom).

On-DNA validation

Due to the large complexity of DELs, there is only limited opportunity to track the efficiency of individual reactions during library synthesis. Therefore, BBs need to pass validation before being used in library synthesis settings. For these bifunctional amino esters, we performed a three-step validation where they were first attached to carboxylic acid functionalized DNA headpiece **7a** (first reverse amidation). Next, the ester was hydrolyzed to obtain acid **9**, and finally, a second reverse amidation with aniline afforded **10**.

Both the reverse amidation and the ester hydrolysis were performed following literature protocols [70,71]. In these experiments, compounds **6b** and **6i** proved to be unstable under on-DNA conditions as they failed to form esters **8b** and **8i**. Closely related structures, such as α-aminobenzothiazol-2-ylacetic acid is known to undergo decarboxylation at room temperature [72]. Compound **8t** underwent decarboxylation during the hydrolysis step. Compounds **6j**, **6l** and **6r** passed validation in moderate to good yields (Scheme 8).

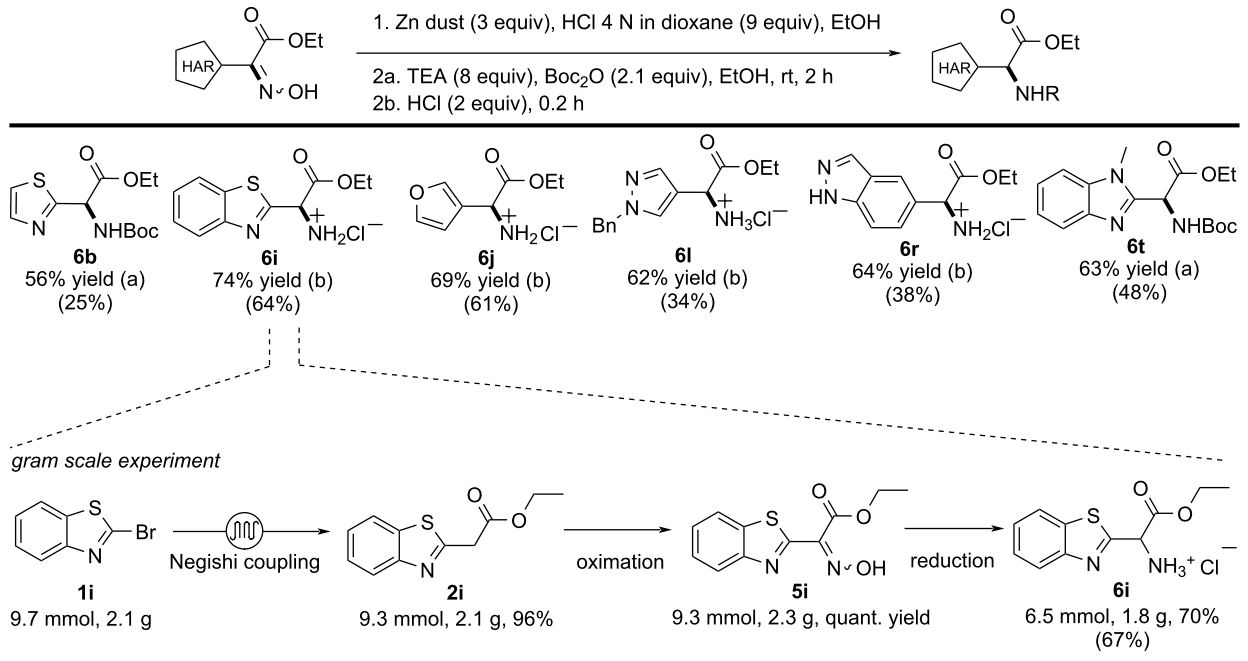

Scheme 7: Amino ester production: general scheme, scope and gram scale experiment. The numbers in brackets represent the overall yield for the synthesis of the amino esters from the Negishi coupling till the reduction/protection step.

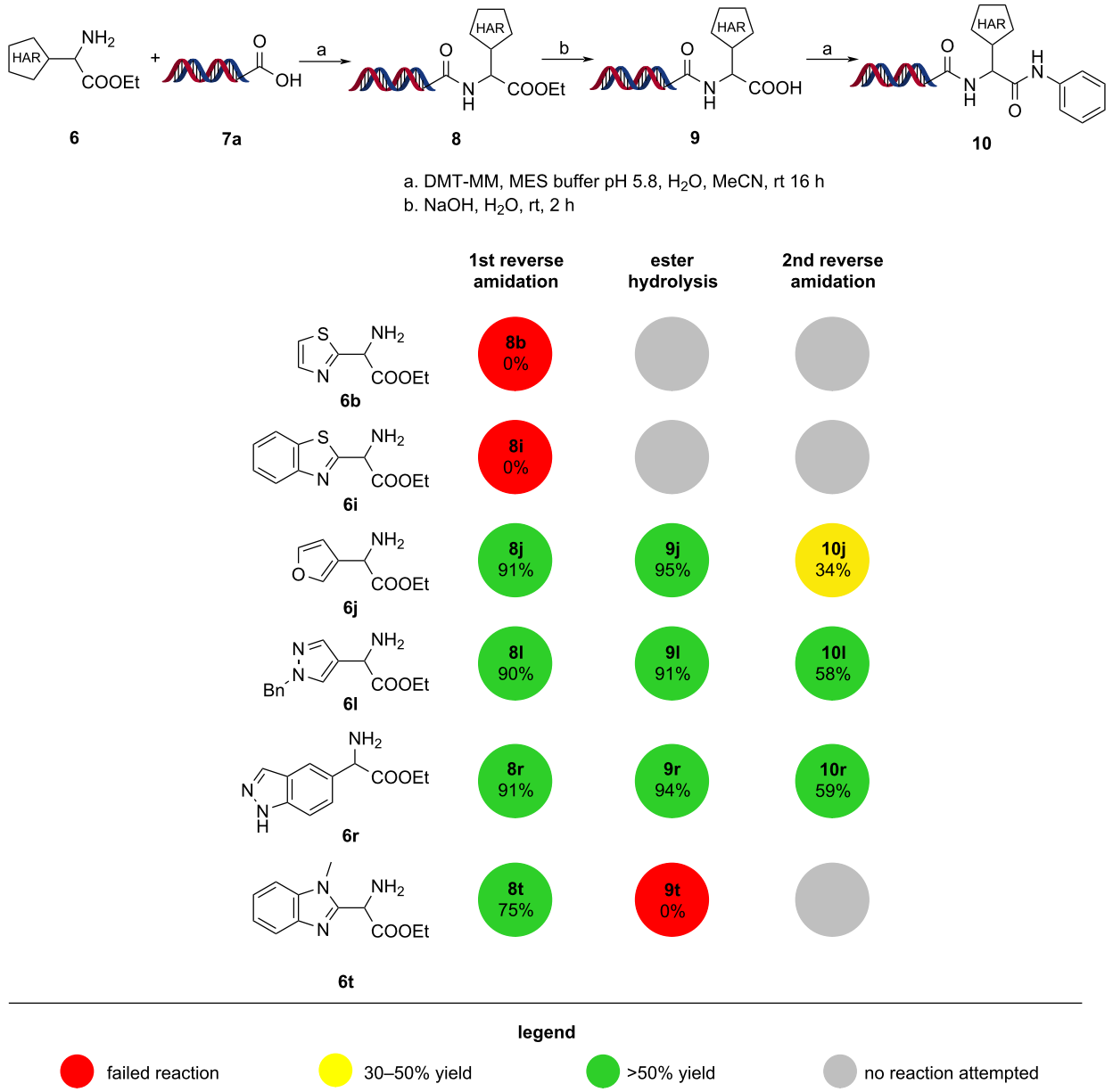

Scheme 8: Reactions scheme and results for the on-DNA experiments. The reported values represent the normalized yield for each reaction (Supporting Information File 1).

Conclusion

In conclusion, by taking advantage of the recent advances in the Negishi cross-coupling reaction we obtained a broad range of heteroarylacetates starting from heteroaromatic halides. One compound from each subclass of medicinal chemistry-relevant substrates (thiazoles, pyrazoles, etc.) was used for the preparation of α-heteroaryl-α-amino esters via the insertion of an oxime group and subsequent reduction step. The procedure relies solely on readily available and widely used reagents, rendering our approach well-suited for both industrial and academic settings. The synthesized amino esters were engaged in a three-step on-DNA validation protocol, demonstrating their possible application for DEL production.

Supporting Information

Supporting Information File 1

Experimental part and NMR spectra.
[https://www.beilstein-journals.org/bjoc/content/supplementary/1860-5397-20-168-S1.pdf]

Acknowledgements

The authors thank Dr. Attila Sveiczer and Dr. Mounir Raji for the consultations and technical support during the practical work of the project, and Dr. Veronika Papp-Kádár for the support during the on-DNA validation experiment. The authors thank Dr. Ying Zhang and Dr. Anthony Keefe for proofreading the manuscript.

Funding

M.G. thanks the European Union for funding under the PhotoReAct Project, H2020 Marie Sklodowska-Curie grant agreement No.956324 (MSCAITN: PhotoReAct).

ORCID® iDs

Matteo Gasparetto - https://orcid.org/0009-0005-9354-6559
Gellért Sipos - https://orcid.org/0000-0001-6956-9009

Data Availability Statement

All data that supports the findings of this study is available in the published article and/or the supporting information to this article.

References

1. Xia, B.; Franklin, G. J.; Lu, X.; Bedard, K. L.; Grady, L. C.; Summerfield, J. D.; Shi, E. X.; King, B. W.; Lind, K. E.; Chiu, C.; Watts, E.; Bodmer, V.; Bai, X.; Marcaurelle, L. A. *ACS Med. Chem. Lett.* **2021,** *12,* 1166–1172. doi:10.1021/acsmedchemlett.1c00156
2. Goodnow, R. A., Jr. *A Handbook for DNA-Encoded Chemistry;* John Wiley & Sons: New York, NY, USA, 2014. doi:10.1002/9781118832738
3. Favalli, N.; Bassi, G.; Scheuermann, J.; Neri, D. *FEBS Lett.* **2018,** *592,* 2168–2180. doi:10.1002/1873-3468.13068
4. Fair, R. J.; Walsh, R. T.; Hupp, C. D. *Bioorg. Med. Chem. Lett.* **2021,** *51,* 128339. doi:10.1016/j.bmcl.2021.128339
5. Fitzgerald, P. R.; Paegel, B. M. *Chem. Rev.* **2021,** *121,* 7155–7177. doi:10.1021/acs.chemrev.0c00789
6. Zhang, Y.; Clark, M. A. *Bioorg. Med. Chem.* **2021,** *41,* 116189. doi:10.1016/j.bmc.2021.116189
7. Geigle, S. N.; Petersen, A. C.; Satz, A. L. *Org. Lett.* **2019,** *21,* 9001–9004. doi:10.1021/acs.orglett.9b03406
8. Wu, G. *Amino Acids* **2009,** *37,* 1–17. doi:10.1007/s00726-009-0269-0
9. Liu, R.; Li, X.; Lam, K. S. *Curr. Opin. Chem. Biol.* **2017,** *38,* 117–126. doi:10.1016/j.cbpa.2017.03.017
10. Clark, M. A.; Acharya, R. A.; Arico-Muendel, C. C.; Belyanskaya, S. L.; Benjamin, D. R.; Carlson, N. R.; Centrella, P. A.; Chiu, C. H.; Creaser, S. P.; Cuozzo, J. W.; Davie, C. P.; Ding, Y.; Franklin, G. J.; Franzen, K. D.; Gefter, M. L.; Hale, S. P.; Hansen, N. J. V.; Israel, D. I.; Jiang, J.; Kavarana, M. J.; Kelley, M. S.; Kollmann, C. S.; Li, F.; Lind, K.; Mataruse, S.; Medeiros, P. F.; Messer, J. A.; Myers, P.; O'Keefe, H.; Oliff, M. C.; Rise, C. E.; Satz, A. L.; Skinner, S. R.; Svendsen, J. L.; Tang, L.; van Vloten, K.; Wagner, R. W.; Yao, G.; Zhao, B.; Morgan, B. A. *Nat. Chem. Biol.* **2009,** *5,* 647–654. doi:10.1038/nchembio.211
11. Strecker, A. *Justus Liebigs Ann. Chem.* **1850,** *75,* 46–51. doi:10.1002/jlac.18500750104
12. Wang, J.; Liu, X.; Feng, X. *Chem. Rev.* **2011,** *111,* 6947–6983. doi:10.1021/cr200057t
13. Mazurkiewicz, R.; Kuźnik, A.; Grymel, M.; Kuźnik, N. *Monatsh. Chem.* **2004,** *135,* 807–815. doi:10.1007/s00706-003-0167-1
14. Dai, Y.; Chen, J.; Wang, Z.; Wang, T.; Wang, L.; Yang, Y.; Qiao, X.; Fan, B. *J. Org. Chem.* **2021,** *86,* 7141–7147. doi:10.1021/acs.joc.1c00426
15. O'Donnell, M. J. *Acc. Chem. Res.* **2004,** *37,* 506–517. doi:10.1021/ar0300625
16. Maruoka, K.; Ooi, T. *Chem. Rev.* **2003,** *103,* 3013–3028. doi:10.1021/cr020020e
17. Dauzonne, D.; Royer, R. *Synthesis* **1987,** 399–401. doi:10.1055/s-1987-27962
18. Corey, E. J.; Link, J. O. *J. Am. Chem. Soc.* **1992,** *114,* 1906–1908. doi:10.1021/ja00031a069
19. Faraggi, T. M.; Rouget-Virbel, C.; Rincón, J. A.; Barberis, M.; Mateos, C.; García-Cerrada, S.; Agejas, J.; de Frutos, O.; MacMillan, D. W. C. *Org. Process Res. Dev.* **2021,** *25,* 1966–1973. doi:10.1021/acs.oprd.1c00208
20. Ni, S.; Garrido-Castro, A. F.; Merchant, R. R.; de Gruyter, J. N.; Schmitt, D. C.; Mousseau, J. J.; Gallego, G. M.; Yang, S.; Collins, M. R.; Qiao, J. X.; Yeung, K.-S.; Langley, D. R.; Poss, M. A.; Scola, P. M.; Qin, T.; Baran, P. S. *Angew. Chem.* **2018,** *130,* 14768–14773. doi:10.1002/ange.201809310
21. Curto, J. M.; Dickstein, J. S.; Berritt, S.; Kozlowski, M. C. *Org. Lett.* **2014,** *16,* 1948–1951. doi:10.1021/ol500506t
22. Bombonato, E.; Fasano, V.; Pecorari, D.; Fornasari, L.; Castagnini, F.; Marcaccio, M.; Ronchi, P. *ACS Omega* **2024,** *9,* 13081–13085. doi:10.1021/acsomega.3c09357
23. Leonard, D. J.; Ward, J. W.; Clayden, J. *Nature* **2018,** *562,* 105–109. doi:10.1038/s41586-018-0553-9
24. Bunch, L.; Krogsgaard-Larsen, P.; Madsen, U. *J. Org. Chem.* **2002,** *67,* 2375–2377. doi:10.1021/jo0162134
25. Jørgensen, C. G.; Clausen, R. P.; Hansen, K. B.; Bräuner-Osborne, H.; Nielsen, B.; Metzler, B.; Kehler, J.; Krogsgaard-Larsen, P.; Madsen, U. *Org. Biomol. Chem.* **2007,** *5,* 463–471. doi:10.1039/b615162k
26. Zhu, S.; Rueping, M. *Chem. Commun.* **2012,** *48,* 11960–11962. doi:10.1039/c2cc36995h
27. Zhu, Z.-Q.; Xiao, L.-J.; Chen, Y.; Xie, Z.-B.; Zhu, H.-B.; Le, Z.-G. *Synthesis* **2018,** *50,* 2775–2783. doi:10.1055/s-0036-1609845
28. Zhu, Z.-Q.; Xiao, L.-J.; Zhou, C.-C.; Song, H.-L.; Xie, Z.-B.; Le, Z.-G. *Tetrahedron Lett.* **2018,** *59,* 3326–3331. doi:10.1016/j.tetlet.2018.07.047
29. Ye, C.-X.; Dansby, D. R.; Chen, S.; Meggers, E. *Nat. Synth.* **2023,** *2,* 645–652. doi:10.1038/s44160-023-00267-w
30. Frühauf, A.; Behringer, M.; Meyer-Almes, F.-J. *Molecules* **2023,** *28,* 5686. doi:10.3390/molecules28155686
31. Wang, Y.-T.; Yang, P.-C.; Zhang, Y.-F.; Sun, J.-F. *Eur. J. Med. Chem.* **2024,** *265,* 116124. doi:10.1016/j.ejmech.2024.116124
32. Polêto, M. D.; Rusu, V. H.; Grisci, B. I.; Dorn, M.; Lins, R. D.; Verli, H. *Front. Pharmacol.* **2018,** *9,* 395. doi:10.3389/fphar.2018.00395
33. Gupta, K.; Sirbaiya, A. K.; Kumar, V.; Rahman, M. A. *Mini-Rev. Med. Chem.* **2022,** *22,* 1895–1935. doi:10.2174/1389557522666220217101805
34. Negishi, E.-i. *Angew. Chem., Int. Ed.* **2011,** *50,* 6738–6764. doi:10.1002/anie.201101380
35. Valente, C.; Belowich, M. E.; Hadei, N.; Organ, M. G. *Eur. J. Org. Chem.* **2010,** 4343–4354. doi:10.1002/ejoc.201000359
36. Wei, B.; Knochel, P. *Synthesis* **2022,** *54,* 246–254. doi:10.1055/a-1589-0150

37. Cossy, J., Ed. *Organozinc Derivatives and Transition Metal Catalysts: Formation of C-C Bonds by Cross-coupling;* De Gruyter: Berlin, Germany, 2023. doi:10.1515/9783110728859
38. Haas, D.; Hammann, J. M.; Greiner, R.; Knochel, P. *ACS Catal.* **2016,** *6,* 1540–1552. doi:10.1021/acscatal.5b02718
39. Muzammil; Zahoor, A. F.; Parveen, B.; Javed, S.; Akhtar, R.; Tabassum, S. *Chem. Pap.* **2024,** *78,* 3399–3430. doi:10.1007/s11696-024-03369-7
40. Abdiaj, I.; Cañellas, S.; Dieguez, A.; Linares, M. L.; Pijper, B.; Fontana, A.; Rodriguez, R.; Trabanco, A.; Palao, E.; Alcázar, J. *J. Med. Chem.* **2023,** *66,* 716–732. doi:10.1021/acs.jmedchem.2c01646
41. Abdiaj, I.; Fontana, A.; Gomez, M. V.; de la Hoz, A.; Alcázar, J. *Angew. Chem., Int. Ed.* **2018,** *57,* 8473–8477. doi:10.1002/anie.201802656
42. Alonso, N.; Miller, L. Z.; Muñoz, J. d. M.; Alcázar, J.; McQuade, D. T. *Adv. Synth. Catal.* **2014,** *356,* 3737–3741. doi:10.1002/adsc.201400243
43. Abdiaj, I.; Huck, L.; Mateo, J. M.; de la Hoz, A.; Gomez, M. V.; Díaz-Ortiz, A.; Alcázar, J. *Angew. Chem., Int. Ed.* **2018,** *57,* 13231–13236. doi:10.1002/anie.201808654
44. Berton, M.; Huck, L.; Alcázar, J. *Nat. Protoc.* **2018,** *13,* 324–334. doi:10.1038/nprot.2017.141
45. PhotoCube - ThalesNano. https://thalesnano.com/products-and-services/photocube/ (accessed May 29, 2024).
46. Capaldo, L.; Wen, Z.; Noël, T. *Chem. Sci.* **2023,** *14,* 4230–4247. doi:10.1039/d3sc00992k
47. Vázquez-Amaya, L. Y.; Coppola, G. A.; Van der Eycken, E. V.; Sharma, U. K. *J. Flow Chem.* **2024,** *14,* 257–279. doi:10.1007/s41981-024-00312-5
48. Zondag, S. D. A.; Mazzarella, D.; Noël, T. *Annu. Rev. Chem. Biomol. Eng.* **2023,** *14,* 283–300. doi:10.1146/annurev-chembioeng-101121-074313
49. Buglioni, L.; Raymenants, F.; Slattery, A.; Zondag, S. D. A.; Noël, T. *Chem. Rev.* **2022,** *122,* 2752–2906. doi:10.1021/acs.chemrev.1c00332
50. Wei, X.-J.; Abdiaj, I.; Sambiagio, C.; Li, C.; Zysman-Colman, E.; Alcázar, J.; Noël, T. *Angew. Chem.* **2019,** *131,* 13164–13168. doi:10.1002/ange.201906462
51. Bonciolini, S.; Pulcinella, A.; Leone, M.; Schiroli, D.; Ruiz, A. L.; Sorato, A.; Dubois, M. A. J.; Gopalakrishnan, R.; Masson, G.; Della Ca', N.; Protti, S.; Fagnoni, M.; Zysman-Colman, E.; Johansson, M.; Noël, T. *Nat. Commun.* **2024,** *15,* 1509. doi:10.1038/s41467-024-45804-z
52. Feng, M.; Tinelli, R.; Meyrelles, R.; González, L.; Maryasin, B.; Maulide, N. *Angew. Chem., Int. Ed.* **2023,** *62,* e202212399. doi:10.1002/anie.202212399
53. Cecere, G.; König, C. M.; Alleva, J. L.; MacMillan, D. W. C. *J. Am. Chem. Soc.* **2013,** *135,* 11521–11524. doi:10.1021/ja406181e
54. Liu, Y.; Zhang, Z.; Ran, F.; Guo, K.; Chen, X.; Zhao, G. *Bioorg. Chem.* **2020,** *97,* 103671. doi:10.1016/j.bioorg.2020.103671
55. Laufer, R.; Ng, G.; Liu, Y.; Patel, N. K. B.; Edwards, L. G.; Lang, Y.; Li, S.-W.; Feher, M.; Awrey, D. E.; Leung, G.; Beletskaya, I.; Plotnikova, O.; Mason, J. M.; Hodgson, R.; Wei, X.; Mao, G.; Luo, X.; Huang, P.; Green, E.; Kiarash, R.; Lin, D. C.-C.; Harris-Brandts, M.; Ban, F.; Nadeem, V.; Mak, T. W.; Pan, G. J.; Qiu, W.; Chirgadze, N. Y.; Pauls, H. W. *Bioorg. Med. Chem.* **2014,** *22,* 4968–4997. doi:10.1016/j.bmc.2014.06.027
56. Lopchuk, J. M.; Hughes, R. P.; Gribble, G. W. *Org. Lett.* **2013,** *15,* 5218–5221. doi:10.1021/ol402385v
57. Cantillo, D.; de Frutos, O.; Rincon, J. A.; Mateos, C.; Kappe, C. O. *J. Org. Chem.* **2014,** *79,* 223–229. doi:10.1021/jo402409k
58. Saito, T.; Saheki, N.; Hatanaka, M.; Ishimaru, T. *J. Heterocycl. Chem.* **1983,** *20,* 73–75. doi:10.1002/jhet.5570200117
59. Zhang, Q.; Zhao, C.; Zhang, X.; He, C.; Pang, S. *New J. Chem.* **2022,** *46,* 1489–1493. doi:10.1039/d1nj05510k
60. Hrib, N. J.; Jurcak, J. G.; Burgher, K. L.; Conway, P. G.; Hartman, H. B.; Kerman, L. L.; Roehr, J. E.; Woods, A. T. *J. Med. Chem.* **1994,** *37,* 2308–2314. doi:10.1021/jm00041a009
61. Baruah, P. K.; Dinsmore, J.; King, A. M.; Salomé, C.; De Ryck, M.; Kaminski, R.; Provins, L.; Kohn, H. *Bioorg. Med. Chem.* **2012,** *20,* 3551–3564. doi:10.1016/j.bmc.2012.04.002
62. Desmarchelier, A.; Ortiz, P.; Harutyunyan, S. R. *Chem. Commun.* **2015,** *51,* 703–706. doi:10.1039/c4cc06719c
63. Angeles-Dunham, V. V.; Nickerson, D. M.; Ray, D. M.; Mattson, A. E. *Angew. Chem., Int. Ed.* **2014,** *53,* 14538–14541. doi:10.1002/anie.201408613
64. Ramalingan, C.; Park, Y.-T. *J. Org. Chem.* **2007,** *72,* 4536–4538. doi:10.1021/jo070297k
65. Paine, J. B., III; Brough, J. R.; Buller, K. K.; Erikson, E. E. *J. Org. Chem.* **1987,** *52,* 3986–3993. doi:10.1021/jo00227a009
66. Jnaneshwara, G. K.; Sudalai, A.; Deshpande, V. H. *J. Chem. Res., Synop.* **1998,** 160–161. doi:10.1039/a705957d
67. Garg, N. K.; Sarpong, R.; Stoltz, B. M. *J. Am. Chem. Soc.* **2002,** *124,* 13179–13184. doi:10.1021/ja027822b
68. Günther, M.; Lategahn, J.; Juchum, M.; Döring, E.; Keul, M.; Engel, J.; Tumbrink, H. L.; Rauh, D.; Laufer, S. *J. Med. Chem.* **2017,** *60,* 5613–5637. doi:10.1021/acs.jmedchem.7b00316
69. Coutant, E. P.; Hervin, V.; Gagnot, G.; Ford, C.; Baatallah, R.; Janin, Y. L. *Beilstein J. Org. Chem.* **2018,** *14,* 2853–2860. doi:10.3762/bjoc.14.264
70. Du, H.-C.; Simmons, N.; Faver, J. C.; Yu, Z.; Palaniappan, M.; Riehle, K.; Matzuk, M. M. *Org. Lett.* **2019,** *21,* 2194–2199. doi:10.1021/acs.orglett.9b00497
71. Satz, A. L.; Cai, J.; Chen, Y.; Goodnow, R.; Gruber, F.; Kowalczyk, A.; Petersen, A.; Naderi-Oboodi, G.; Orzechowski, L.; Strebel, Q. *Bioconjugate Chem.* **2015,** *26,* 1623–1632. doi:10.1021/acs.bioconjchem.5b00239
72. Baudet, P.; Otten, C. *Helv. Chim. Acta* **1970,** *53,* 1683–1693. doi:10.1002/hlca.19700530715

BEILSTEIN JOURNAL OF ORGANIC CHEMISTRY

Development of a flow photochemical process for a π-Lewis acidic metal-catalyzed cyclization/radical addition sequence: in situ-generated 2-benzopyrylium as photoredox catalyst and reactive intermediate

Masahiro Terada*[1], Zen Iwasaki[1], Ryohei Yazaki[1], Shigenobu Umemiya[1] and Jun Kikuchi[1,2]

Full Research Paper

Open Access

Address:
[1]Department of Chemistry, Graduate School of Science, Tohoku University, Aoba-ku, Sendai 980-8578, Japan and [2]Graduate School of Pharmaceutical Science, Tohoku University, Aoba-ku, Sendai 980-8578, Japan

Email:
Masahiro Terada* - mterada@tohoku.ac.jp

* Corresponding author

Keywords:
2-benzopyrylium; flow chemistry; isocromene; photochemical reaction; π-Lewis acidic metal

Beilstein J. Org. Chem. **2024,** *20,* 1973–1980.
https://doi.org/10.3762/bjoc.20.173

Received: 27 March 2024
Accepted: 30 July 2024
Published: 13 August 2024

This article is part of the thematic issue "Photocatalysis and photochemistry in organic synthesis".

Guest Editor: T. Noël

Abstract

A flow photochemical reaction system for a π-Lewis acidic metal-catalyzed cyclization/radical addition sequence was developed, which utilizes in situ-generated 2-benzopyrylium intermediates as the photoredox catalyst and electrophilic substrates. The key 2-benzopyrylium intermediates were generated in the flow reaction system through the intramolecular cyclization of *ortho*-carbonyl alkynylbenzene derivatives by the π-Lewis acidic metal catalyst $AgNTf_2$ and the subsequent proto-demetalation with trifluoroacetic acid. The 2-benzopyrylium intermediates underwent further photoreactions with benzyltrimethylsilane derivatives as the donor molecule in the flow photoreactor to provide 1*H*-isochromene derivatives in higher yields in most cases than the batch reaction system.

Introduction

Flow chemistry has been actively studied in recent years as a method to run a reaction continuously using a flow path or tube, rather than in a flask [1-16]. This method has attracted much attention because, unlike a batch reaction system, it allows for rapid generation of unstable chemical species by controlling parameters such as flow velocity and mixing properties, and in some cases makes it possible to achieve reactions that are difficult to perform using batch chemistry [17-21]. In general, efficient two-phase mixing and heat transfer, as well as ease of scale-up, are the advantages of using a flow system. In addition, reproducibility in a liquid–liquid flow system is improved because the flow velocity and temperature can be precisely con-

trolled by using a syringe pump and a temperature control unit, respectively. Moreover, as the reaction mixture continues to flow and the reaction can be quenched immediately when necessary, the decomposition of an unstable product under the reaction conditions can be avoided [22-25]. Furthermore, when a photoreaction is performed in a flow system, there is an advantage that the light irradiation efficiency [26-29] is increased. Thus, the flow photochemical process is crucial and beneficial to product formation.

Recently, we reported a sequential transformation consisting of a π-Lewis acidic metal-catalyzed cyclization [30-45] and subsequent photochemical radical addition [46-54], which affords 1*H*-isochromene derivatives **3** through three catalytic cycles (Scheme 1a) [55]: catalytic cycles I and II and a photoredox cycle of the photocatalyst [56,57] (see Supporting Information File 1 for the overall catalytic cycles). In catalytic cycle I, the key cationic components, 2-benzopyrylium intermediates **A**, are generated in situ by the activation of the alkyne moiety of *ortho*-carbonyl alkynylbenzene derivatives **1** in the presence of the π-Lewis acidic metal catalyst [M]X [$AgNTf_2$ or $Cu(NTf_2)_2$] and subsequent intramolecular cyclization followed by protodemetalation with trifluoroacetic acid (TFA). In catalytic cycle II, photoexcitation of the generated 2-benzopyrylium intermediates **A** under light irradiation facilitates single-electron transfer (SET) from benzyltrimethylsilane derivatives **2** as the donor molecule, initiating further radical reactions through the formation of radical cations **B**. Nucleophilic arylmethyl radicals **C**, which are generated from radical cations **B** by desilylation, undergo an addition reaction with 2-benzopyrylium intermediates **A**, giving rise to the corresponding radical cation. Catalytic cycle II is completed through a SET from **D**, a reduced form of the photoredox catalyst 2-benzopyrylium intermediates **A**, to the generated radical cation, affording 1*H*-isochromene derivatives **3**. The photoredox cycle is also completed with the regeneration of cations **A** through SET from **D**.

The most distinctive feature of this sequential transformation is that the in situ-generated 2-benzopyrylium intermediates **A** are used not only as an electrophile but also as a photoredox catalyst. However, as this reaction is carried out under relatively harsh conditions (i.e., light irradiation, use of an excess amount of TFA), the stability of products **3** was a concern. Indeed, subjecting product **3a** to the optimal reaction conditions with either $AgNTf_2$ or $Cu(NTf_2)_2$ resulted in the significant degradation of **3a**, although the degradation of **3a** was partially suppressed when $AgNTf_2$ was used (Scheme 1b). Accordingly, we envisioned that the characteristics of the flow photochemical process, i.e., efficient light irradiation and immediate separation of the formed product from the reaction system, would be suitable for this sequential reaction. Here, we report the results of our investigation on the use of a flow photochemical reaction system to improve the yield of the present sequential transformation.

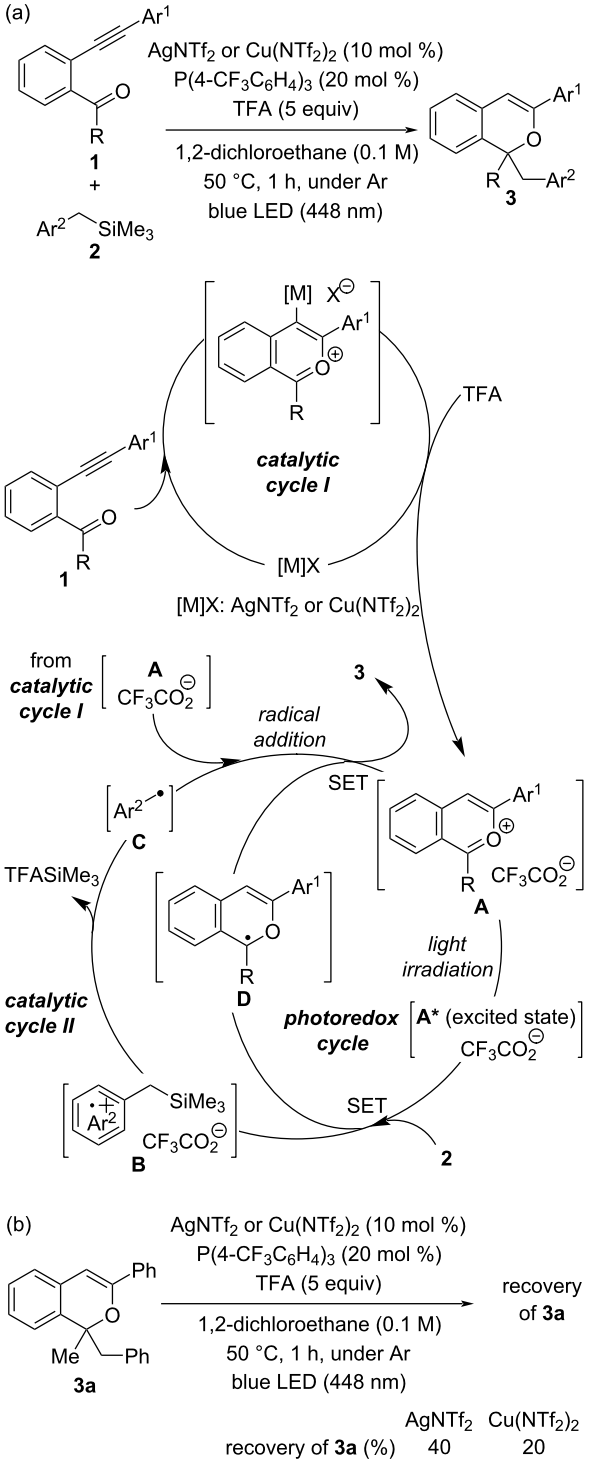

Scheme 1: (a) Sequential π-Lewis acidic metal-catalyzed cyclization/photochemical radical addition for the formation of 1*H*-isochromene derivatives **3** and its plausible catalytic cycles. (b) Stability of **3a** under the optimal reaction conditions of the batch reaction.

Results and Discussion

At the outset of our studies to optimize the flow reaction conditions, we employed $AgNTf_2$ as the π-Lewis acidic metal catalyst because of its high solubility in 1,2-dichloroethane (1,2-DCE) [58] and ability to partially suppress the degradation of the product formed (Scheme 1b). When designing a flow reaction system for the present sequential transformation, we considered the fact that the transformation involves three catalytic cycles. In particular, given that catalytic cycle I (see Scheme 1a) generates, e.g., key cationic components, 2-benzopyrylium intermediates **A** without light irradiation, it is necessary to ensure that the reaction time of catalytic cycle I is not affected by the timescale of the flow reaction. Therefore, we adopted a dual syringe system in which two solutions are mixed before being introduced into the photoreactor (volume: 1.0 mL) (Table 1, top right). After several trials, we decided to fill syringe A with *o*-alkynylacetophenone **1a** and syringe B with $AgNTf_2$, $P(4\text{-}CF_3C_6H_4)_3$, benzyltrimethylsilane (**2a**, TMSBn), and TFA (see Supporting Information File 1 for details). At this time, the volumes of the solutions placed in the two syringes were adjusted to be approximately the same. The initial conditions of the flow reaction were based on those of the batch reaction [0.1 mmol of **1a**, 10 μmol (10 mol %) of $AgNTf_2$, 20 μmol (20 mol %) of $P(4\text{-}CF_3C_6H_4)_3$, 1.0 mmol (10 equiv) of **2a**, and 0.5 mmol (5 equiv) of TFA under light irradiation (blue LED: λ_{max} = 448 nm) at 50 °C for 1 h in 1 mL (total volume) of 1,2-DCE] [55] with a flow rate of 3 mL/h (light irradiation time: 20 min in the flow reaction, 1 h in the batch reaction). As shown in Table 1, product **3a** was obtained in moderate yield (entry 1: 42%, cf. batch reaction: 76%). Lowering the reaction temperature to 25 °C reduced the yield (Table 1, entry 2: 35%), but decreasing the amount of the phosphine ligand from 20 mol % to 5 mol % markedly improved the yield (Table 1, entry 3: 53%). Even when the flow rate was increased from 3 mL/h to 24 mL/h (light irradiation time was shortened from 20 min to 2.5 min), the yield of **3a** was maintained (Table 1, entry 4: 53%). Under these conditions, no improvement in yield was observed when the premixing zone (0.7 mL) was provided

Table 1: Screening of reaction conditions in the flow reaction system[a].

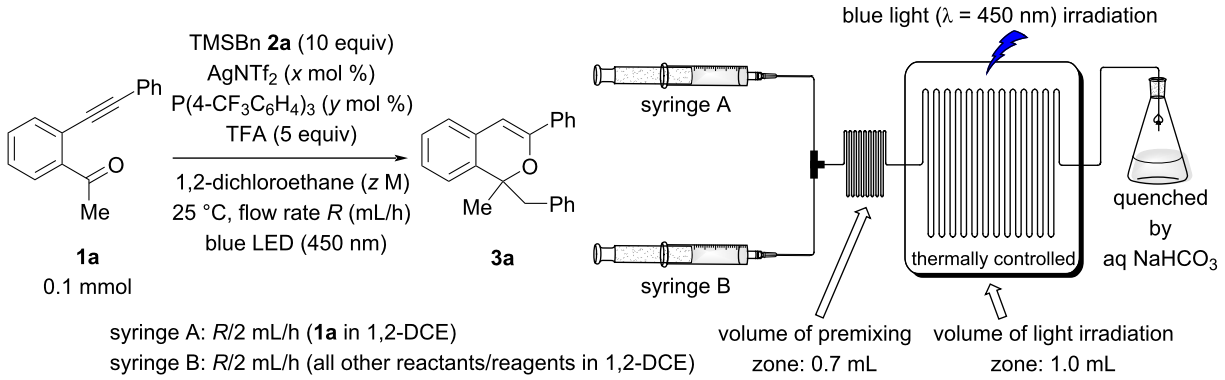

Entry	$AgNTf_2$ (*x* mol %)	$P(4\text{-}CF_3C_6H_4)_3$ (*y* mol %)	Conc. of **1a** (*z* M)	Flow rate (*R* mL/h)	Premixing zone (mL)	Yield of **3a** (%)[b]	Recovery of **1a** (%)[b]
1[c]	10	20	0.1	3	none	42	0
2	10	20	0.1	3	none	35	22
3	10	5	0.1	3	none	53	1
4	10	5	0.1	24	none	53	0
5	10	5	0.1	24	0.7	52	9
6	5	2.5	0.1	24	none	26	14
7	5	2.5	0.1	24	0.7	49	0
8	5	2.5	0.05	24	0.7	61	0
9	2	1	0.05	24	0.7	28	28
10[d]	5	2.5	0.05	24	0.7	77	0

[a]Unless otherwise noted, all reactions were carried out in a flow photochemical reactor (volume: 1.0 mL, λ_{max} = 450 nm) using a dual syringe system, as shown in the table scheme. Syringe A: 0.1 mmol of **1a** in 1,2-DCE (0.55 mL). Syringe B: $AgNTf_2$, $P(4\text{-}CF_3C_6H_4)_3$, TMSBn (**2a**), and TFA in 1,2-DCE (0.45 mL); [b]Yield was determined by NMR analysis using 1,1,2,2-tetrabromoethane as an internal standard; [c]At 50 °C. [d]Reaction was conducted on a 0.5 mmol scale. Syringe A: 0.5 mmol of **1a** in 1,2-DCE (5.4 mL). Syringe B: 25 μmol (5 mol %) of $AgNTf_2$, 12.5 μmol (2.5 mol %) of $P(4\text{-}CF_3C_6H_4)_3$, 5 mmol (10 equiv) of TMSBn (**2a**), and 2.5 mmol (5 equiv) of TFA in 1,2-DCE (4.6 mL).

(Table 1, entry 5: 52%); however, the effect of adding the premixing zone was remarkable when the amount of $AgNTf_2$ was reduced by half (5 mol %; Table 1, entry 6 vs entry 7: 26% vs 49%). These results suggest that the generation of 2-benzopyrylium intermediates **A**, (i.e., catalytic cycle I) requires a certain reaction time (at this flow rate: ca. 2 min). Moreover, the yield of **3a** was improved when the concentration of **1a** was lowered from 0.1 M to 0.05 M (Table 1, entry 8: 61%). Meanwhile, further reducing the catalyst loading from 5 mol % to 2 mol % resulted in a significant decrease in yield (Table 1, entry 9: 28%). When the reaction was scaled up from 0.1 mmol to 0.5 mmol of **1a** in consideration of the dead volume of the flow reactor, the product **3a** was obtained in markedly improved yield (Table 1, entry 10: 77%) [59] which was comparable to that of the batch reaction (76%). Notably, however, the present flow reaction was performed at 25 °C (batch: 50 °C) with half the amount of $AgNTf_2$ (flow: 5 mol %, batch: 10 mol %), and the light irradiation time was shortened to only 2.5 minutes (batch: 1 h). Thus, under the optimal conditions (Table 1, entry 10), the flow reaction system proved extremely useful for improving the efficiency of the present photochemical sequential transformation.

With the optimal flow reaction conditions in hand, we next investigated the scope of substrates **1** by introducing a series of substituents to the terminal phenyl group. The results of the batch reaction system are also shown for comparison in Table 2 (right-hand side) [55]. As expected, the use of the flow reaction system significantly increased yields, although the yields obtained in the reactions of substrates having an electron-donating methoxy group were low to moderate regardless of the substitution pattern (Table 2, entries 1, 2, and 6). Indeed, when a methoxy group was introduced at the *para*-position, product **3b** was obtained in low yield (Table 2, entry 1: 14%). Because this yield was lower than that obtained in the batch reaction (48%), the flow reaction conditions for **1b** were thoroughly reconsidered (see Supporting Information File 1 for details). As a result, extending the premixing time and the light irradiation time

Table 2: Scope of substrates[a].

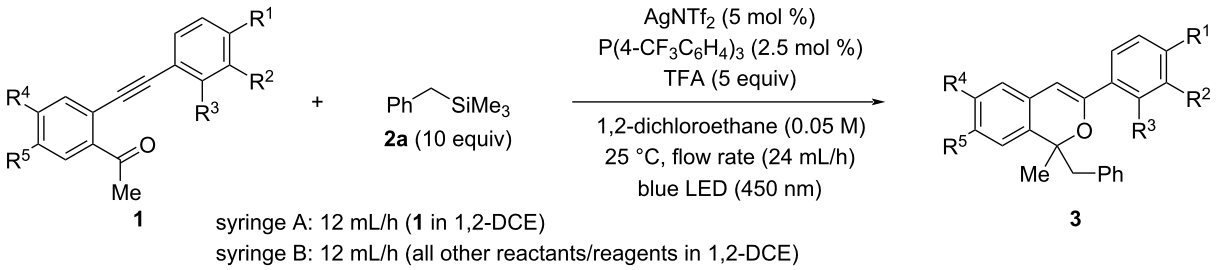

Entry	1	R^1	R^2	R^3	R^4	R^5	3	Yield of 3 (%)[b]	Batch reaction using $AgNTf_2$. Yield of 3 (%)[b,c]
1	**1b**	MeO	H	H	H	H	**3b**	14	48[d]
2[e]	**1b**						**3b**	54	
3	**1c**	Me	H	H	H	H	**3c**	76	21
4	**1d**	Br	H	H	H	H	**3d**	57	10
5	**1e**	CF_3	H	H	H	H	**3e**	77	65
6	**1f**	H	MeO	H	H	H	**3f**	39	40
7	**1g**	H	Me	H	H	H	**3g**	75	50
8	**1h**	H	Br	H	H	H	**3h**	68	63
9	**1i**	H	CF_3	H	H	H	**3i**	65	42
10	**1j**	H	H	Me	H	H	**3j**	76	72
11	**1k**	H	H	H	F	H	**3k**	79	–
12	**1l**	H	H	H	H	F	**3l**	75	–

[a]Unless otherwise noted, all reactions were carried out in the flow photochemical reactor (volume: 1.0 mL, λ_{max} = 450 nm) having a 0.7 mL premixing zone using a dual syringe system with a flow rate of 24 mL/h (12 mL/h for each syringe) at 25 °C. Syringe A: 0.5 mmol of **1** in 1,2-DCE (5.4 mL). Syringe B: 25 μmol (5 mol %) of $AgNTf_2$, 12.5 μmol (2.5 mol %) of $P(4\text{-}CF_3C_6H_4)_3$, 5 mmol (10 equiv) of TMSBn (**2a**), and 2.5 mmol (5 equiv) of TFA in 1,2-DCE (4.6 mL). [b]Yield was determined by NMR analysis using 1,1,2,2-tetrabromoethane as an internal standard. Substrates **1** were not recovered in all cases. All products **3** were isolated before structural assignment. [c]Batch reaction conditions (see ref. [55]): Unless otherwise noted, all reactions were carried out using blue LED (λ_{max} = 448 nm), 0.1 mmol of **1**, 1.0 mmol (10 equiv) of TMSBn (**2a**), 10 μmol (10 mol %) of $AgNTf_2$, 20 μmol (20 mol %) of $P(4\text{-}CF_3C_6H_4)_3$, and 5 equiv of TFA in 1,2-DCE (1.0 mL: 0.1 M of **1**) at 50 °C for 1 h. [d]At 0 °C for 6 h. [e]The flow photochemical reactor having a 1.1 mL premixing zone using a dual syringe system with a flow rate of 6 mL/h (3 mL/h for each syringe).

(Table 2, entry 2) led to an improved yield; the obtained yield was higher than that of the batch reaction system even when half the amount of $AgNTf_2$ was used with the temperature reduced to 25 °C (flow: 54% vs batch: 48%). Meanwhile, the reaction of substrate **1c** having a methyl group as a weak electron-donating group at the *para*-position afforded product **3c** in high yield (Table 2, entry 3: 76%). In addition, the reaction of **1d** having a bromo group resulted in a moderate yield, but with a significant improvement compared with the batch reaction (Table 2, entry 4: 57% vs 10%). The reaction of **1e** substituted with a strong electron-withdrawing trifluoromethyl group afforded the product **3e** in high yield (Table 2, entry 5: 77%), again confirming the high efficiency of the flow reaction system (batch: 54%). Next, the effects of the substituent at the *meta*-position were investigated. Substrate **1f** having a methoxy group afforded compound **3f** in only moderate yield (Table 2, entry 6: 39%), similar to the batch reaction (40%). The reactions of substrates having a methyl, bromo, or trifluoromethyl group gave the corresponding products **3g**–**i**, respectively, in good yields (Table 2, entries 7–9). The *ortho*-methyl-substituted substrate **1j** was also compatible, affording product **3j** in good yield (Table 2, entry 10: 76%). This yield was comparable to that of the substrate having a methyl group at the *para*- or *meta*-position, despite the steric hindrance of the *ortho*-substituent (Table 2, entry 10 vs entries 3 and 7). When a fluoro group was introduced to the tethering phenyl backbone, a high yield was obtained regardless of whether it was introduced at the 6- or 7-position (Table 2, entries 11 and 12).

Next, the effects of a carbonyl substituent, instead of a methyl ketone substituent, were investigated (Table 3). First, the reaction was performed with phenyl ketone **1m**, but product **3m** was obtained in low yield (Table 3, entry 1: 7%). This yield was lower than that obtained in the batch reaction (30%), and because 28% of **1m** were recovered, the flow reaction conditions were further examined (see Supporting Information File 1 for details). Although the yield of **3m** was improved to 19% (Table 3, entry 2) by increasing the temperature of the premixing zone from room temperature to 50 °C and reducing the flow rate from 24 mL/h to 6 mL/h (light irradiation time was extended from 2.5 min to 10 min), it did not exceed the yield of the batch reaction. In contrast, aldehyde **1n** having a simple phenyl group gave product **3n** in good yield (Table 3, entry 3: 72%). Because the yield of this flow reaction was better than that of the batch reaction (65%), the reactions of aldehydes with a series of substituents introduced to the terminal phenyl group were further investigated (Table 3, entries 4–7). Aldehydes having an electron-donating methyl group and an electron-with-

Table 3: Sequential transformation of phenyl ketone **1m** and aldehydes **1n**–**r**[a].

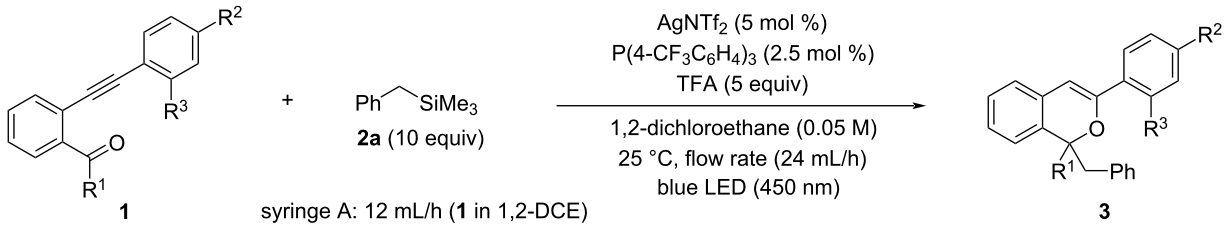

Entry	**1**	R^1	R^2	R^3	**3**	Yield of **3** (%)[b]	Recovery of **1** (%)[b]	Batch reaction using $AgNTf_2$. Yield of **3** (%)[c]
1	**1m**	Ph	H	H	**3m**	7	29	30
2[d,e]	**1m**				**3m**	19	0	
3	**1n**	H	H	H	**3n**	72	0	65[f]
4	**1o**	H	Me	H	**3o**	82	5	–
5	**1p**	H	Br	H	**3p**	75	0	34[f]
6	**1q**	H	CF_3	H	**3q**	63	18	–
7[e]	**1r**	H	H	Me	**3r**	73	8	–

[a]Unless otherwise noted, all reactions were carried out in the flow photochemical reactor (volume: 1.0 mL, λ_{max} = 450 nm) having a 0.7 mL premixing zone using a dual syringe system with a flow rate of 24 mL/h (12 mL/h for each syringe) at 25 °C. Syringe A: 0.5 mmol of **1** in 1,2-DCE (5.4 mL). Syringe B: 25 μmol (5 mol %) of $AgNTf_2$, 12.5 μmol (2.5 mol %) of $P(4\text{-}CF_3C_6H_4)_3$, 5 mmol (10 equiv) of TMSBn (**2a**), and 2.5 mmol (5 equiv) of TFA in 1,2-DCE (4.6 mL). [b]Yield was determined by NMR analysis using 1,1,2,2-tetrabromoethane as an internal standard. All products **3** were isolated before structural assignment. [c]Batch reaction conditions: unless otherwise noted, reactions were carried out using 0.1 mmol of **1**, 1.0 mmol (10 equiv) of TMSBn (**2a**), 10 μmol (10 mol %) of $AgNTf_2$, 20 μmol (20 mol %) of $P(4\text{-}CF_3C_6H_4)_3$, and 5 equiv of TFA in 1,2-DCE (1 mL: 0.1 M of **1**) at 50 °C for 1 h. [d]The flow photochemical reactor having a 0.5 mL premixing zone using a dual syringe system with a flow rate of 6 mL/h (3 mL/h for each syringe). [e]The temperature of the premixing zone was increased to 50 °C. [f]The reaction was performed using 0.05 M of **1** and 2.5 equiv of TFA for 2 h.

drawing bromo group at the *para*-position of the phenyl moiety gave products **3o** and **3p**, respectively, in high yields (Table 3, entries 4 and 5). The aldehyde **1q** bearing a strong electron-withdrawing trifluoromethyl group at the *para*-position gave product **3q** in moderate yield (Table 3, entry 6: 63%), with the recovery of substrate **1q** (18%). The reaction of *ortho*-methyl-substituted aldehyde **1r** afforded the product **3r** in high yield when the temperature of the premixing zone was increased to 50 °C (Table 3, entry 7: 73%).

The scope of donor molecules **2b** and **2c** having an electron-withdrawing trifluoromethyl group and an electron-donating methoxy group [60,61] at the *para*-position of the benzyltrimethylsilane, respectively, was also investigated in the present flow reaction system (Scheme 2). As expected, the flow reaction of **2b** having a trifluoromethyl group afforded product **3s** in higher yield (50%) than that of the batch reaction (18%) under the optimal reaction conditions. In contrast, in the flow reaction of **2c** having a methoxy group, product **3t** was obtained in a markedly lower yield (32%) than that of the batch reaction (54%). However, extending the light irradiation time by reducing the flow rate from 24 mL/h to 6 mL/h (light irradiation time: 24 mL/h = 2.5 min, 6 mL/h = 10 min) significantly improved the yield of **3t** (78%), presumably because of the retardation of the desilylation process (from **B** to **C** in Scheme 1a).

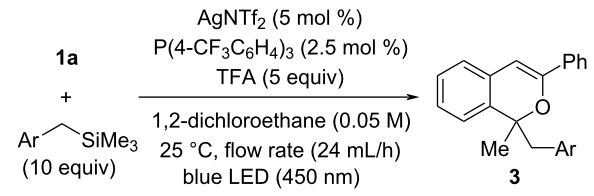

2b: Ar = 4-$CF_3C_6H_4$-
2c: Ar = 4-$MeOC_6H_4$-

syringe A: 12 mL/h (**1a** in 1,2-DCE)
syringe B: 12 mL/h (all other reactants/reagents in 1,2-DCE)

	yield of **3** (%)	flow reaction	cf. batch reaction (ref. [55])
3s: Ar = 4-$CF_3C_6H_4$-	50		18
3t: Ar = 4-$MeOC_6H_4$-	32 (78)[a]		54

Scheme 2: The reaction with benzyltrimethylsilane derivatives **2**.
[a]Flow rate was 6 mL/h and premixing zone was 0.2 mL.

Conclusion

We have demonstrated a flow reaction system for a π-Lewis acidic metal-catalyzed cyclization/photochemical radical addition sequence, affording, in most cases, the 1*H*-isochromene derivatives in higher yields than the batch reaction system, even with the amount of the π-Lewis acidic metal catalyst reduced by half. In the present sequential transformation, the key cationic species, 2-benzopyrylium intermediates, were generated in situ through the $AgNTf_2$-catalyzed intramolecular cyclization of *ortho*-carbonyl alkynylbenzene derivatives and subsequent proto-demetalation with TFA. Further photoreactions of 2-benzopyrylium intermediates with benzyltrimethylsilane derivatives as the donor molecule were conducted in the flow photoreactor. We confirmed that the flow reaction system is an excellent method for improving the efficiency of the present sequential transformation, avoiding product degradation under photochemical reaction conditions. Further investigation of other flow photochemical reactions using in situ-generated organic cations is in progress in our laboratory.

Supporting Information

Supporting Information File 1

The exploratory investigation, experimental procedures, and characterization data.
[https://www.beilstein-journals.org/bjoc/content/supplementary/1860-5397-20-173-S1.pdf]

Supporting Information File 2

Copies of NMR spectra.
[https://www.beilstein-journals.org/bjoc/content/supplementary/1860-5397-20-173-S2.pdf]

Funding

This work was partially supported by a Grant-in-Aid for Scientific Research on Innovative Areas “Hybrid Catalysis for Enabling Molecular Synthesis on Demand” (JP17H06447) and a Grant-in-Aid for Transformative Research Areas (A) “Green Catalysis Science for Renovating Transformation of Carbon-Based Resources” (JP23H04908) from MEXT, Japan and a Grant-in-Aid for Young Scientists (JP19K15552) from JSPS.

Author Contributions

Masahiro Terada: conceptualization; funding acquisition; methodology; project administration; resources; supervision; visualization; writing – original draft; writing – review & editing. Zen Iwasaki: data curation; formal analysis; investigation; validation; visualization. Ryohei Yazaki: data curation; formal analysis; investigation. Shigenobu Umemiya: data curation; formal analysis; investigation; methodology; supervision; writing – review & editing. Jun Kikuchi: conceptualization; funding acquisition; investigation; methodology; project administration; supervision; visualization; writing – review & editing.

ORCID® iDs

Masahiro Terada - https://orcid.org/0000-0002-0554-8652
Shigenobu Umemiya - https://orcid.org/0000-0002-1793-856X
Jun Kikuchi - https://orcid.org/0000-0001-9892-8832

Data Availability Statement

All data that supports the findings of this study is available in the published article and/or the supporting information to this article.

References

1. Ehrfeld, W.; Hessel, V.; Löwe, H. *Microreactors;* Wiley-VCH: Weinheim, Germany, 2000. doi:10.1002/3527601953
2. Yoshida, J. *Basics of Flow Microreactor Synthesis;* Springer: Tokyo, Japan, 2015. doi:10.1007/978-4-431-55513-1
3. Noël, T., Ed. *Organometallic Flow Chemistry;* Topics in Organometallic Chemistry, Vol. 57; Springer International Publishing: Cham, Switzerland, 2016. doi:10.1007/978-3-319-33243-7
4. Mason, B. P.; Price, K. E.; Steinbacher, J. L.; Bogdan, A. R.; McQuade, D. T. *Chem. Rev.* **2007,** *107,* 2300–2318. doi:10.1021/cr050944c
5. Ahmed-Omer, B.; Brandt, J. C.; Wirth, T. *Org. Biomol. Chem.* **2007,** *5,* 733–740. doi:10.1039/b615072a
6. Watts, P.; Wiles, C. *Chem. Commun.* **2007,** 443–467. doi:10.1039/b609428g
7. McMullen, J. P.; Jensen, K. F. *Annu. Rev. Anal. Chem.* **2010,** *3,* 19–42. doi:10.1146/annurev.anchem.111808.073718
8. Yoshida, J.; Kim, H.; Nagaki, A. *ChemSusChem* **2011,** *4,* 331–340. doi:10.1002/cssc.201000271
9. Wiles, C.; Watts, P. *Green Chem.* **2012,** *14,* 38–54. doi:10.1039/c1gc16022b
10. Kirschning, A.; Kupracz, L.; Hartwig, J. *Chem. Lett.* **2012,** *41,* 562–570. doi:10.1246/cl.2012.562
11. McQuade, D. T.; Seeberger, P. H. *J. Org. Chem.* **2013,** *78,* 6384–6389. doi:10.1021/jo400583m
12. Elvira, K. S.; i Solvas, X. C.; Wootton, R. C. R.; deMello, A. J. *Nat. Chem.* **2013,** *5,* 905–915. doi:10.1038/nchem.1753
13. Pastre, J. C.; Browne, D. L.; Ley, S. V. *Chem. Soc. Rev.* **2013,** *42,* 8849–8869. doi:10.1039/c3cs60246j
14. Cambié, D.; Bottecchia, C.; Straathof, N. J. W.; Hessel, V.; Noël, T. *Chem. Rev.* **2016,** *116,* 10276–10341. doi:10.1021/acs.chemrev.5b00707
15. Plutschack, M. B.; Pieber, B.; Gilmore, K.; Seeberger, P. H. *Chem. Rev.* **2017,** *117,* 11796–11893. doi:10.1021/acs.chemrev.7b00183
16. Buglioni, L.; Raymenants, F.; Slattery, A.; Zondag, S. D. A.; Noël, T. *Chem. Rev.* **2022,** *122,* 2752–2906. doi:10.1021/acs.chemrev.1c00332
17. Nagaki, A.; Kim, H.; Yoshida, J. *Angew. Chem., Int. Ed.* **2008,** *47,* 7833–7836. doi:10.1002/anie.200803205
18. Kim, H.; Min, K.-I.; Inoue, K.; Im, D. J.; Kim, D.-P.; Yoshida, J. *Science* **2016,** *352,* 691–694. doi:10.1126/science.aaf1389
19. Seo, H.; Katcher, M. H.; Jamison, T. F. *Nat. Chem.* **2017,** *9,* 453–456. doi:10.1038/nchem.2690
20. Otake, Y.; Nakamura, H.; Fuse, S. *Angew. Chem., Int. Ed.* **2018,** *57,* 11389–11393. doi:10.1002/anie.201803549
21. Nagaki, A.; Yamashita, H.; Hirose, K.; Tsuchihashi, Y.; Yoshida, J. *Angew. Chem., Int. Ed.* **2019,** *58,* 4027–4030. doi:10.1002/anie.201814088
22. Nagaki, A.; Ichinari, D.; Yoshida, J. *Chem. Commun.* **2013,** *49,* 3242–3244. doi:10.1039/c3cc40392k
23. Moon, S.-Y.; Jung, S.-H.; Bin Kim, U.; Kim, W.-S. *RSC Adv.* **2015,** *5,* 79385–79390. doi:10.1039/c5ra14890a
24. Degennaro, L.; Maggiulli, D.; Carlucci, C.; Fanelli, F.; Romanazzi, G.; Luisi, R. *Chem. Commun.* **2016,** *52,* 9554–9557. doi:10.1039/c6cc04588j
25. Nauth, A. M.; Lipp, A.; Lipp, B.; Opatz, T. *Eur. J. Org. Chem.* **2017,** 2099–2103. doi:10.1002/ejoc.201601394
26. Tucker, J. W.; Zhang, Y.; Jamison, T. F.; Stephenson, C. R. J. *Angew. Chem., Int. Ed.* **2012,** *51,* 4144–4147. doi:10.1002/anie.201200961
27. Hernandez-Perez, A. C.; Collins, S. K. *Angew. Chem., Int. Ed.* **2013,** *52,* 12696–12700. doi:10.1002/anie.201306920
28. Elliott, L. D.; Knowles, J. P.; Koovits, P. J.; Maskill, K. G.; Ralph, M. J.; Lejeune, G.; Edwards, L. J.; Robinson, R. I.; Clemens, I. R.; Cox, B.; Pascoe, D. D.; Koch, G.; Eberle, M.; Berry, M. B.; Booker-Milburn, K. I. *Chem. – Eur. J.* **2014,** *20,* 15226–15232. doi:10.1002/chem.201404347
29. Talla, A.; Driessen, B.; Straathof, N. J. W.; Milroy, L.-G.; Brunsveld, L.; Hessel, V.; Noël, T. *Adv. Synth. Catal.* **2015,** *357,* 2180–2186. doi:10.1002/adsc.201401010
30. Asao, N.; Nogami, T.; Takahashi, K.; Yamamoto, Y. *J. Am. Chem. Soc.* **2002,** *124,* 764–765. doi:10.1021/ja017366b
31. Yao, T.; Zhang, X.; Larock, R. C. *J. Am. Chem. Soc.* **2004,** *126,* 11164–11165. doi:10.1021/ja0466964
32. Patil, N. T.; Yamamoto, Y. *Chem. Rev.* **2008,** *108,* 3395–3442. doi:10.1021/cr050041j
33. Rudolph, M.; Hashmi, A. S. K. *Chem. Commun.* **2011,** *47,* 6536–6544. doi:10.1039/c1cc10780a
34. Shiroodi, R. K.; Gevorgyan, V. *Chem. Soc. Rev.* **2013,** *42,* 4991–5001. doi:10.1039/c3cs35514d
35. Saito, K.; Kajiwara, Y.; Akiyama, T. *Angew. Chem., Int. Ed.* **2013,** *52,* 13284–13288. doi:10.1002/anie.201308303
36. Obradors, C.; Echavarren, A. M. *Chem. Commun.* **2014,** *50,* 16–28. doi:10.1039/c3cc45518a
37. Terada, M.; Li, F.; Toda, Y. *Angew. Chem., Int. Ed.* **2014,** *53,* 235–239. doi:10.1002/anie.201307371
38. Dorel, R.; Echavarren, A. M. *Chem. Rev.* **2015,** *115,* 9028–9072. doi:10.1021/cr500691k
39. Debrouwer, W.; Heugebaert, T. S. A.; Roman, B. I.; Stevens, C. V. *Adv. Synth. Catal.* **2015,** *357,* 2975–3006. doi:10.1002/adsc.201500520
40. Asiri, A. M.; Hashmi, A. S. K. *Chem. Soc. Rev.* **2016,** *45,* 4471–4503. doi:10.1039/c6cs00023a
41. Lauder, K.; Toscani, A.; Scalacci, N.; Castagnolo, D. *Chem. Rev.* **2017,** *117,* 14091–14200. doi:10.1021/acs.chemrev.7b00343
42. Zhang, Z.; Smal, V.; Retailleau, P.; Voituriez, A.; Frison, G.; Marinetti, A.; Guinchard, X. *J. Am. Chem. Soc.* **2020,** *142,* 3797–3805. doi:10.1021/jacs.9b11154
43. Raj, A. S. K.; Narode, A. S.; Liu, R.-S. *Org. Lett.* **2021,** *23,* 1378–1382. doi:10.1021/acs.orglett.1c00038
44. Greiner, L. C.; Arichi, N.; Inuki, S.; Ohno, H. *Angew. Chem., Int. Ed.* **2023,** *62,* e202213653. doi:10.1002/anie.202213653
45. Das, S. *Asian J. Org. Chem.* **2023,** *12,* e202300267. doi:10.1002/ajoc.202300267
46. Beatty, J. W.; Douglas, J. J.; Cole, K. P.; Stephenson, C. R. J. *Nat. Commun.* **2015,** *6,* 7919. doi:10.1038/ncomms8919
47. Nakajima, K.; Miyake, Y.; Nishibayashi, Y. *Acc. Chem. Res.* **2016,** *49,* 1946–1956. doi:10.1021/acs.accounts.6b00251

48. Ermanis, K.; Colgan, A. C.; Proctor, R. S. J.; Hadrys, B. W.; Phipps, R. J.; Goodman, J. M. *J. Am. Chem. Soc.* **2020,** *142,* 21091–21101. doi:10.1021/jacs.0c09668
49. Xiong, T.; Zhang, Q. *Chem. Soc. Rev.* **2021,** *50,* 8857–8873. doi:10.1039/d1cs00208b
50. Alfonzo, E.; Hande, S. M. *ACS Catal.* **2020,** *10,* 12590–12595. doi:10.1021/acscatal.0c03851
51. Kikuchi, J.; Kodama, S.; Terada, M. *Org. Chem. Front.* **2021,** *8,* 4153–4159. doi:10.1039/d1qo00657f
52. Schlegel, M.; Qian, S.; Nicewicz, D. A. *ACS Catal.* **2022,** *12,* 10499–10505. doi:10.1021/acscatal.2c02997
53. Takemura, N.; Sumida, Y.; Ohmiya, H. *ACS Catal.* **2022,** *12,* 7804–7810. doi:10.1021/acscatal.2c01964
54. Miura, T.; Yoritate, M.; Hirai, G. *Chem. Commun.* **2023,** *59,* 8564–8567. doi:10.1039/d3cc02361c
55. Terada, M.; Yazaki, R.; Obayashi, R.; Iwasaki, Z.; Umemiya, S.; Kikuchi, J. *Chem. Sci.* **2024,** *15,* 6115–6121. doi:10.1039/d4sc00808a
56. Prier, C. K.; Rankic, D. A.; MacMillan, D. W. C. *Chem. Rev.* **2013,** *113,* 5322–5363. doi:10.1021/cr300503r
57. Romero, N. A.; Nicewicz, D. A. *Chem. Rev.* **2016,** *116,* 10075–10166. doi:10.1021/acs.chemrev.6b00057
58. $Cu(NTf_2)_2$ which was also the effective catalyst in our batch system (ref. [55]) did not solve well in 1,2-DCE.
59. Benzyltrimethylsilane (**2a**), which was not consumed in the corresponding radical reaction, was almost completely recovered.
60. Maruyama, T.; Mizuno, Y.; Shimizu, I.; Suga, S.; Yoshida, J. *J. Am. Chem. Soc.* **2007,** *129,* 1902–1903. doi:10.1021/ja068589a
61. Montanaro, S.; Ravelli, D.; Merli, D.; Fagnoni, M.; Albini, A. *Org. Lett.* **2012,** *14,* 4218–4221. doi:10.1021/ol301900p

License and Terms

BEILSTEIN JOURNAL OF ORGANIC CHEMISTRY

Photoredox-catalyzed intramolecular nucleophilic amidation of alkenes with β-lactams

Valentina Giraldi[‡1,2], Giandomenico Magagnano[‡1], Daria Giacomini[1,2], Pier Giorgio Cozzi[1,2] and Andrea Gualandi[*1,2]

Full Research Paper

Open Access

Address:
[1]Department of Chemistry “G. Ciamician”, ALMA MATER STUDIORUM - Università di Bologna, Via Gobetti 85, 40129 Bologna, Italy and [2]Center for Chemical Catalysis - C3, ALMA MATER STUDIORUM - Università di Bologna, Via Gobetti 85, 40129 Bologna, Italy

Email:
Andrea Gualandi[*] - andrea.gualandi10@unibo.it

* Corresponding author ‡ Equal contributors

Keywords:
β-lactam; acridinium photocatalyst; alkenes; amides; intramolecular radical reaction; photoredox catalysis

Beilstein J. Org. Chem. **2024,** *20,* 2461–2468.
https://doi.org/10.3762/bjoc.20.210

Received: 23 July 2024
Accepted: 19 September 2024
Published: 01 October 2024

This article is part of the thematic issue "Photocatalysis and photochemistry in organic synthesis".

Guest Editor: T. Noël

Abstract

The direct nucleophilic addition of amides to unfunctionalized alkenes via photoredox catalysis represents a facile approach towards functionalized alkylamides. Unfortunately, the scarce nucleophilicity of amides and competitive side reactions limit the utility of this approach. Herein, we report an intramolecular photoredox cyclization of alkenes with β-lactams in the presence of an acridinium photocatalyst. The approach uses an intramolecular nucleophilic addition of the β-lactam nitrogen atom to the radical cation photogenerated in the linked alkene moiety, followed by hydrogen transfer from the hydrogen atom transfer (HAT) catalyst. This process was used to successfully prepare 2-alkylated clavam derivatives.

Introduction

Access to nitrogen radicals for the functionalization of alkenes is a field under active investigation [1-4], as it gives the possibility to directly introduce nitrogen into an alkyl chain (alkene carboamination) to obtain valuable nitrogen-containing molecules [5,6]. Among several N-centered radicals, such as aminyl, amidyl, or iminyl radicals, N-heterocyclic amidyl radicals were largely underinvestigated despite their importance as intermediates or relevant N-heterocyclic products in medicinal chemistry [7-10].

Recently, photoredox catalysis has emerged as a novel area of research [11,12], particularly focusing on innovative approaches to synthesize natural or bioactive compounds [13]. In the carboamination of alkenes, amides are used in photoredox cyclizations under proton-coupled electron transfer (PCET) conditions [14-17]. An alternative method to generate *N*-amidyl radicals uses activated N–O amide derivatives capable of generating amidyl radicals through fragmentation [18,19]. The direct formation of amidyl radicals in the presence of a carbon alkyl

chain could lead to a competitive 1,5-hydrogen atom transfer (1,5-HAT) [20-22], limiting the direct functionalization of amides with alkenes under photoredox conditions. Another viable approach for amide functionalization through photoredox catalysis involves the nucleophilic addition, in the presence of base, of an amide to a radical cation obtained by oxidation of an unfunctionalized alkene moiety (Figure 1A) [23-25]. The nucleophilic attack of the nitrogen atom on the oxidized C=C double bond results in the formation of a radical intermediate after deprotonation. This radical intermediate can proceed through various pathways (e.g., HAT, oxidation) to yield the desired final product.

In the functionalization of amides with alkenes under oxidative conditions, the oxidation potential of the alkene plays a pivotal role in the oxidation to a radical cation through photoredox catalysis [26]. Alkenes that are less functionalized possess a higher oxidation potential, necessitating the use of potent photocatalysts (PC) that act as oxidants in the excited state [27]. The direct functionalization of amides with alkenes has been a relatively underexplored area in research, as evidenced by the limited number of examples reported in the literature. An interesting observation was made by the Nicewicz group during their investigation of the hydrofunctionalization reaction of unsaturated amides and thioamides [28]. They have found that the oxygen atom of the amide group, rather than the nitrogen atom, acted as a nucleophile, leading to the formation of 2-oxazolines and 2-thiazolines. Another recent example of intramolecular nucleophilic attack induced by photocatalytic oxidation was reported by Yoon et al. with tosylamide derivatives [29]. Specifically, amides were employed in a photoredox cyclization process using a strong photooxidative acridinium catalyst such as the Fukuzumi catalyst (**I**, Figure 1B) [30,31]. Through tailored molecular design, it is possible to enhance the oxidation capability of these catalysts, enabling the utilization of less reactive alkenes and even aromatic molecules such as toluene [32].

Until now, heterocyclic amides such as β-lactam compounds have not been employed in alkene carboaminations. However, photoredox catalysis could be applied to a suitable β-lactam intermediate decorated with an alkene moiety to achieve N–H addition and cyclization to the fused bicyclic system of clavams (Figure 2A).

Clavulanic acid (**1**, Figure 2B) belongs to the family of clavam β-lactam compounds and is well known as a potent β-lactamase inhibitor [33,34]. It is produced by the filamentous bacterium *Streptomyces clavuligerus,* but in low yield. Various clavams **2**–**5** have been identified (Figure 2B), either through isolation as natural metabolites or obtained by synthetic methods [35-43]. The inhibitory activity of β-lactamases is exhibited by those congeners with a (3*R*,5*R*)-configuration, such as clavulanic acid (**1**), whereas clavams with other configurations are not lactamase inhibitors, although some of these have antifungal or antibacterial properties [35]. In the literature, oxacepham scaffolds, the 6-membered fused bicyclic analog of clavams, were prepared from appropriately substituted unfused precursors by

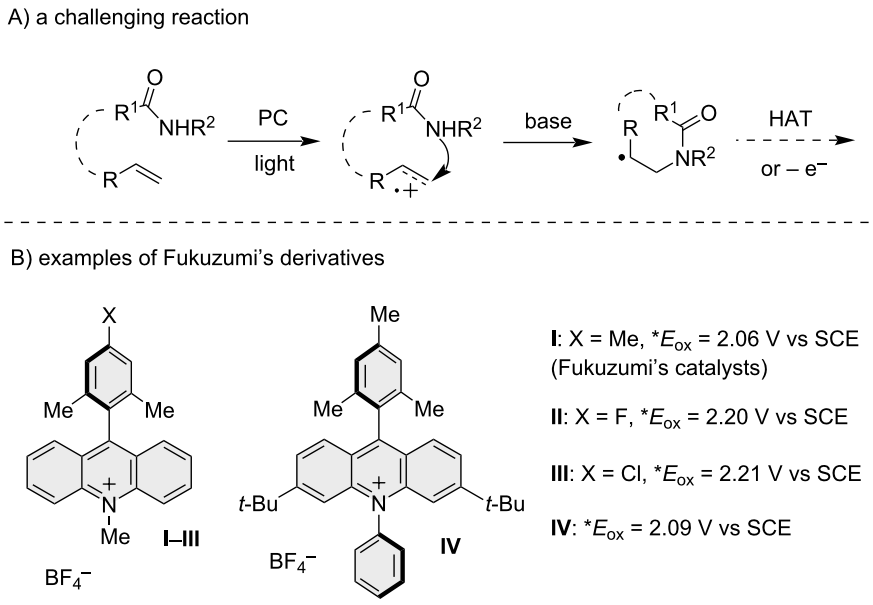

Figure 1: A) Photoredox amidocyclization reaction. B) The strongly oxidizing Fukuzumi catalyst (**I**) used in the functionalization of alkenes by amides, and more recent variants.

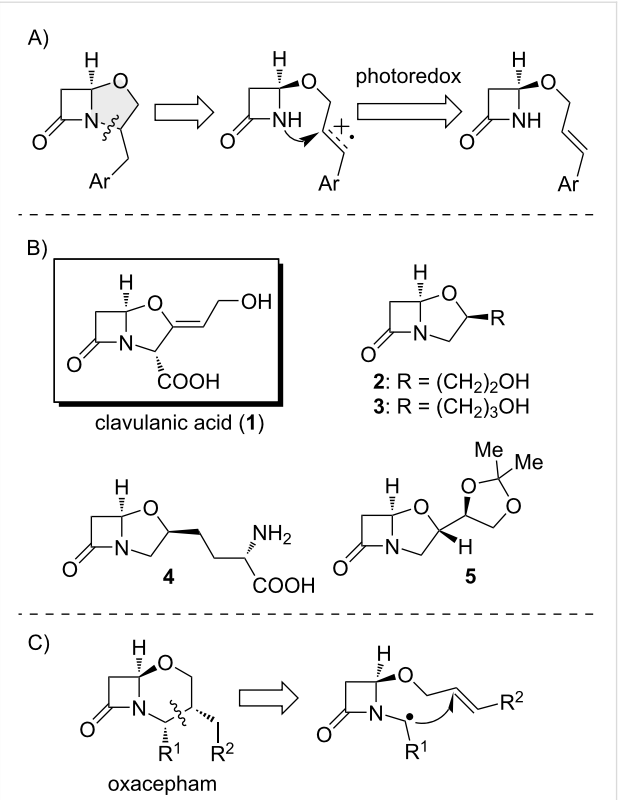

Figure 2: A) Access of clavam derivatives by intramolecular photoredox reaction of alkenes. B) Clavulanic acid and its derivatives. C) Construction of the oxacepham scaffold by radical cyclization.

intramolecular C-radical addition to alkene functionalities [44]. The utilization of radical conditions has prevented the effective nucleophilic opening of the lactams.

Notably, all reported structures have alkyl or aryl substituents in position 3 of the clavam ring. Conversely, clavams substituted with alkyl chains at the 2-position, to the best of our knowledge, have not been previously reported and are absent from common organic compound databases. To explore potential biological effects, a simple and modular approach to these molecules is thus required. Based on this, we decided to use photoredox chemistry to access 2-alkylclavams through a simplified synthetic pathway. We investigated the intramolecular nucleophilic addition of the nitrogen atom of the β-lactams to photooxidized alkenes (Figure 2A), and our findings are presented in this study.

Results and Discussion

The initial phase of our investigation involved the synthesis of suitable starting compounds for the following oxidative cyclization. For this purpose, a series of 4-alkoxy-β-lactams containing an alkene group was readily synthesized starting from commercially available 4-acetoxy-2-azetidinone (**6**) by nucleophilic displacement of the 4-acetoxy group with allylic alcohols promoted by $Zn(OAc)_2$ (see compounds **8a**–**h**, Scheme 1) [45]. Similarly, enantiopure derivatives **10c**–**f** were synthesized from the commercially available β-lactam **9**, a key intermediate for the industrial preparation of carbapenems.

Starting from the reaction conditions reported by Nicewicz and Morse [28], we optimized the conditions with compound **8c** as the model substrate for the photoredox cyclization (Table 1). The reaction was carried out in DCM with acridinium PC **IV** (5 mol %), 50 mol % of PhSSPh as HAT catalyst, and lutidine (50 mol %) as the base.

Upon 72 hours of irradiation with a blue light at 456 nm, the product **11c** was obtained in a satisfactory yield as a mixture of diastereoisomers in a 1.4:1 ratio (Table 1, entry 1). Assignment of the relative configurations as *cis* or *trans* was achieved by

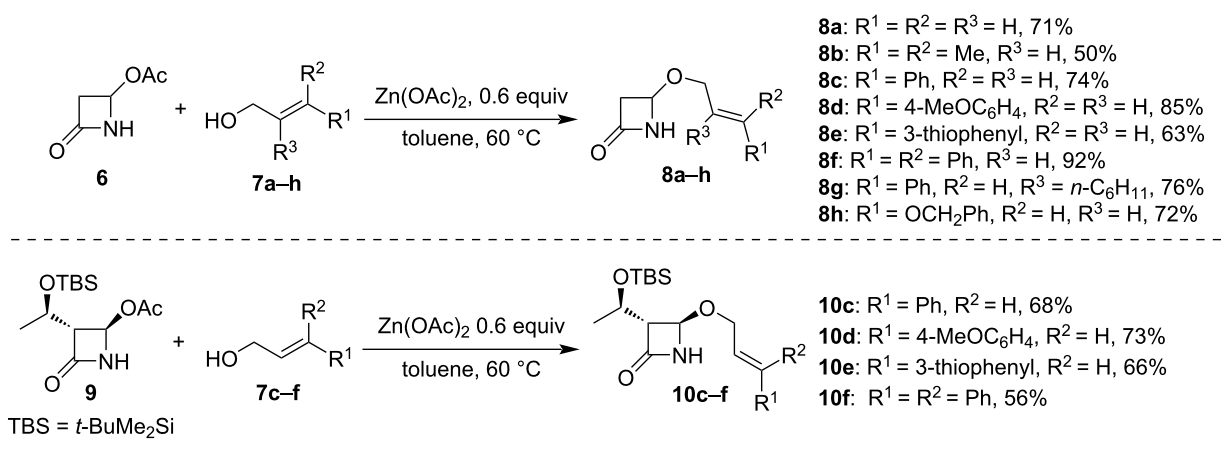

Scheme 1: Preparation of alkenyl β-lactam derivatives for the intramolecular photoredox reaction.

Table 1: Intramolecular cyclization of β-lactams induced by photoredox conditions.[a]

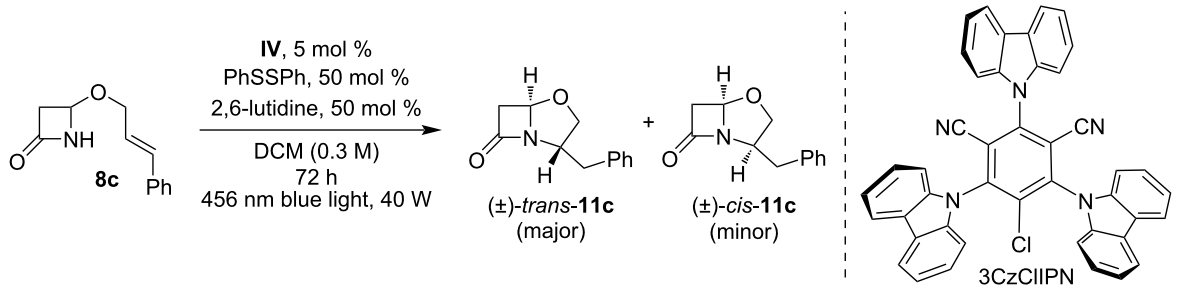

entry	deviation from standard conditions	conversion to **11c**, %[b,c]	dr[d]
1	—	72 (70)	1.4:1
2	absence of **IV**	0	—
3	absence of light	0	—
4	reaction time 14 h	traces	—
5	20 mol % PhSSPh, 20 mol % 2,6-lutidine	49	1.4:1
6	DMF solvent	0	—
7	MeCN solvent	68	1.4:1
8	DCE solvent	49	1.4:1
9	**I** instead of **IV**	60	1.4:1
10	3CzClIPN instead of **IV**	0	—

[a]The reactions were conducted under irradiation with a Kessil blue light (40 W) for 72 hours on a 0.05 mmol scale. [b]Conversion determined by ^{1}H NMR analysis of the crude reaction mixture. [c]In parentheses: isolated yield after purification by flash column chromatography. [d]*Trans*/*cis* dr determined by ^{1}H NMR analysis on the crude reaction mixture.

^{1}H NMR analysis, considering the chemical shifts of the proton in the α-position of the β-lactam nitrogen atom and the geminal protons in the benzylic position (see Supporting Information File 1). The difference in the chemical shifts of these protons in the two isomers could be attributed to the influence of the anisotropy of the neighboring carboxy group of the β-lactam and could be correlated with the configuration at the bridgehead stereocenter [46]. This analysis revealed the preferred formation of the *trans*- over the *cis*-isomer.

The optimal PC for the reaction was acridinium salt **IV** (Table 1, entry 1), while the Fukuzumi catalyst (**I**), commonly employed by Nicewicz et al., was less effective (Table 1, entry 9). 3CzClIPN, an organic dye belonging to the class of thermally activated delayed fluorescence (TADF) dyes commonly employed nowadays in photoredox catalysis [47], was tested in our reaction. This dye was chosen due to its oxidizing properties, and it ranks among the most oxidizing agents within this class of compounds ($E_{1/2}$[*PC/PC$^{\bullet-}$] = +1.56 V vs SCE) [48], but it proved ineffective in our reaction (Table 1, entry 10). The reaction was successfully conducted in various solvents, such as DCM, DCE, and MeCN (Table 1, entries 1, 7, and 8). However, DMF failed to yield the desired product (Table 1, entry 6). Shortening the reaction time to 14 hours resulted in minimal product formation (Table 1, entry 4), while reducing the amount of PhSSPh and lutidine to 20 mol % led to a lower yield (Table 1, entry 5).

With the optimized reaction conditions in hand, we submitted the previously prepared 4-alkoxy-β-lactam substrates **8a**–**h** to photoredox conditions (Scheme 1), and the salient results are reported in Scheme 2. Unfortunately, the substrates **8a**,**b** displayed low reactivity due to their significantly higher oxidation potential compared to the excited photoredox catalysts (>2.5 V vs SCE) [49]. However, other derivatives exhibited a satisfactory product yield ranging from moderate to good. Substrate **8d** exhibited an enhancement in reaction diastereoselectivity, resulting in the isolation of product **11d** with a dr of 6.7:1 in favor of the *trans*-diastereoisomer. Remarkably, the formation of a fully substituted quaternary center was possible, as observed for the product **11g**, where the *trans*-diastereoisomer was favored.

In this study, enantiopure 3-(1'-(*tert*-butyldimethylsilyl)ethyl)-β-lactams **10c**–**f** were also tested. Products **12c**–**f** were obtained with moderate to good yield, underscoring the feasibility of the methodology for the C3-substituted β-lactam moiety. The configuration at the newly formed stereocenter in the five-membered ring was attributed by ^{1}H NMR analysis for **11c**. Moreover, the configuration was also confirmed by NOE studies on

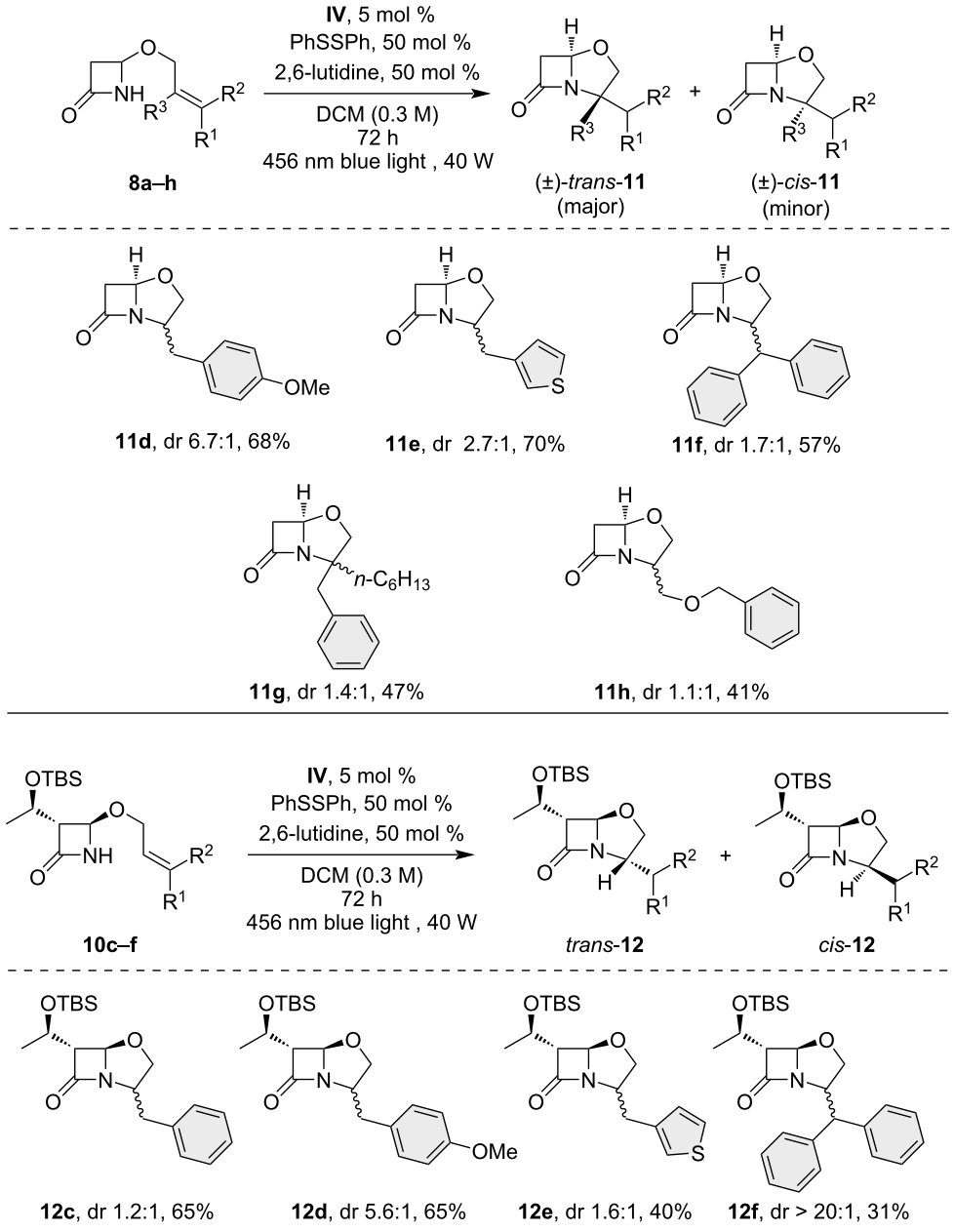

Scheme 2: Photoredox-catalyzed intramolecular N-alkylation reactions of various β-lactams. The *trans*/*cis* dr was determined by ^{1}H NMR analysis of the crude reaction mixture.

the two isolated diastereoisomers, which confirmed the preferred *trans*-isomer formation (see Supporting Information File 1).

Analysis of the dr values revealed that the diastereoselectivity of the nucleophilic attack of the β-lactam on the radical cationic intermediate was influenced by stereoelectronic factors. Compounds unsubstituted at position C-3 of the β-lactam ring, **11d**–**h**, showed modest stereoselectivity with a higher dr (6.7:1) for compound **11d**, which has an electron-donating methoxy group on the phenyl substituent. Derivatives with a 3-OTBS side chain, **12c**–**e**, displayed moderate diastereoselectivity, except for the higher diastereoselectivity achieved for **12f** (dr 20:1), probably due to steric effects, albeit at the expense of a reduced isolated yield.

Across all tested substrates, nucleophilic attack predominantly occurred at the homobenzylic position, leading to the regiose-

lective formation of clavam derivative with 2-benzylic substitution due to aryl stabilization of the radical intermediate (see mechanistic discussion below).

We briefly investigated whether this protocol could be adapted to other lactams, allowing for a practical synthesis of bicyclic structures. The resulting bicyclic lactam substrate could serve as a foundation to access pyrroloisoquinoline alkaloids [50,51]. The model substrate **14** was synthesized in a two-step process starting from succinimide (Scheme 3). Through a simple reaction in toluene at 80 °C in the presence of $Zn(OAc)_2$, the hemiaminal derivative **13** underwent substitution with cinnamyl alcohol, resulting in the isolation of **14** with a satisfactory yield. Under optimized reaction conditions, the photocatalytic cyclization occurred by producing *trans*-**15** in 35% yield as the single diastereoisomer.

For the reaction mechanism, we propose a mechanistic hypothesis according to the study by Nicewicz and Nguyen (Figure 3) [23]. The incorporation of electron-donating groups into the acridinium core, as in catalyst **IV**, enhances charge transfer by stabilizing the mesityl moiety. Conversely, the introduction of *tert*-butyl groups increases the life time of the excited state [52-56]. As a consequence, the PC **IV** is a strong oxidant in the excited state and displays unique oxidizing properties ($E_{1/2}$[*PC^+/$PC^\bullet$] = +2.09 V vs SCE) [55,56]. The *PC^+ species can oxidize the unsaturated lactam, thereby producing the corresponding radical cation intermediate **A**. The low stabilization by amide-bond resonance of the cyclic four-membered β-lactam [57,58] ensures a good nucleophilicity of the nitrogen atom to efficiently attack the radical cation **A**, giving the bicyclic radical intermediate **B**. Amide is an ambident nucleophile, and oxygen attack of radical cation **A** is also conceivable to give the corresponding imidate [28]. In our reaction, O-addition is disfavored due to the formation of an unsaturated four-membered ring as

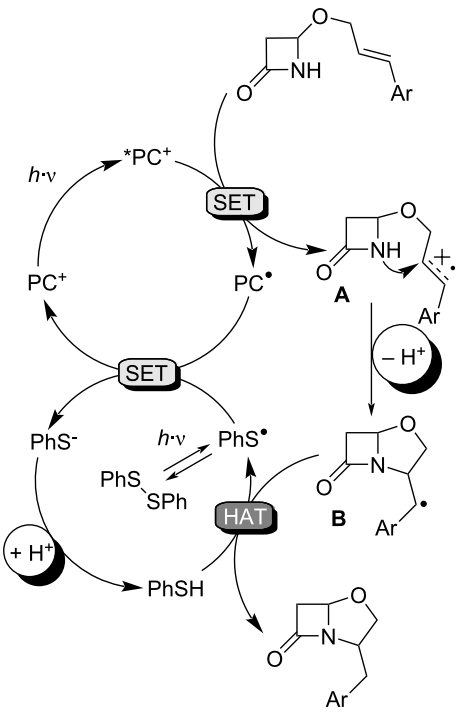

Figure 3: Tentative mechanism for the photo-cyclization reaction.

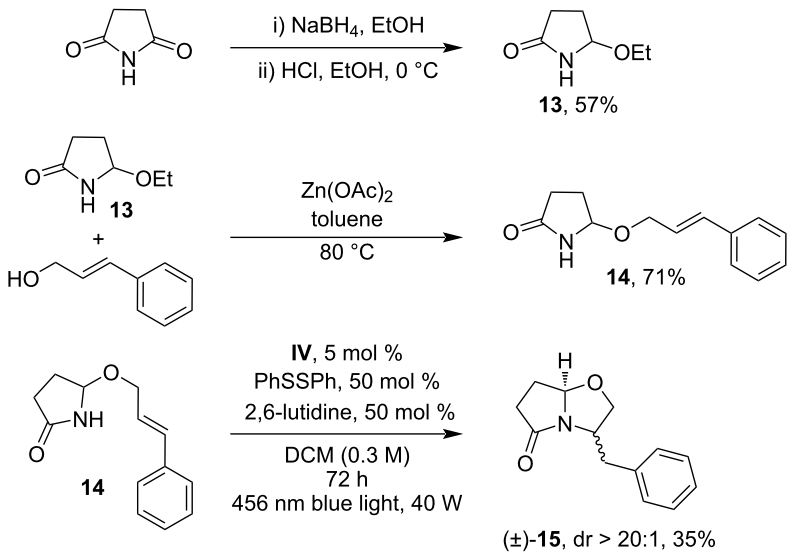

Scheme 3: Synthesis of the model substrate **14** and its photoredox-catalyzed intramolecular N-alkylation reaction. The *trans*/*cis* dr was determined by ^{1}H NMR analysis of the crude reaction mixture.

final product, characterized by significant ring strain [59]. Under light irradiation, PhSSPh is in equilibrium with the corresponding thiyl radical, which is subsequently reduced to thiophenolate by $PC^{\bullet}$, originating from the reduction of $*PC^{+}$. The reduction potential of $PhS^{-}/PhS^{\bullet}$ ($E_{p_{red}}$ = +0.45 V vs SCE) [60,61] is sufficient to oxidize the radical form of **IV** ($PC^{\bullet}/PC^{+}$ = −0.57 V vs SCE) [55,56]. Finally, PhS^{-} is protonated and HAT from thiophenol to **B** furnishes the final product, closing the HAT cycle. Additionally, lutidine acts as a proton shuttle between the lactam NH unit and thiophenolate.

Conclusion

To conclude, we have employed a photoredox methodology to access clavam and pyrrolyloxazole intermediates, showing the possibility of using the nucleophilic nitrogen atom of β-lactams under photoredox conditions. The acridinium catalyst **IV** was able to oxidize the C=C double bond present in the substrates to access the corresponding radical cation. The reaction shows high regioselectivity and good to moderate diastereoselectivity with satisfactory yield. The limitation, which will be further addressed by a more powerful catalyst, is related to the unreactivity of unsubstituted alkenes due to their higher oxidation potential. Biological studies concerning the new derivatives will also be a subject of future investigations.

Supporting Information

Supporting Information File 1

Reaction optimization studies, general experimental procedures, product isolation and characterization, spectroscopic data for new compounds, and copies of NMR spectra.
[https://www.beilstein-journals.org/bjoc/content/supplementary/1860-5397-20-210-S1.pdf]

Funding

P. G. C., D. G., and A. G. acknowledge the University of Bologna for financial support. MIUR national project (PRIN 2017 ID: 20174SYJAF) SURSUMCAT “Raising up Catalysis for Innovative Developments” and European Union’s Horizon 2020 research and innovation program under grant agreement no. 951996 are gratefully acknowledged.

ORCID® iDs

Valentina Giraldi - https://orcid.org/0000-0002-0593-1010
Giandomenico Magagnano - https://orcid.org/0000-0003-4893-4876
Daria Giacomini - https://orcid.org/0000-0001-8038-3926
Pier Giorgio Cozzi - https://orcid.org/0000-0002-2677-101X
Andrea Gualandi - https://orcid.org/0000-0003-2403-4216

Data Availability Statement

All data that supports the findings of this study is available in the published article and/or the supporting information of this article.

References

1. Kwon, K.; Simons, R. T.; Nandakumar, M.; Roizen, J. L. *Chem. Rev.* **2022,** *122,* 2353–2428. doi:10.1021/acs.chemrev.1c00444
2. Wang, P.; Zhao, Q.; Xiao, W.; Chen, J. *Green Synth. Catal.* **2020,** *1,* 42–51. doi:10.1016/j.gresc.2020.05.003
3. Pratley, C.; Fenner, S.; Murphy, J. A. *Chem. Rev.* **2022,** *122,* 8181–8260. doi:10.1021/acs.chemrev.1c00831
4. Gao, S.; Li, F. *Adv. Funct. Mater.* **2023,** *33,* 2304291. doi:10.1002/adfm.202304291
5. Kerru, N.; Gummidi, L.; Maddila, S.; Gangu, K. K.; Jonnalagadda, S. B. *Molecules* **2020,** *25,* 1909. doi:10.3390/molecules25081909
6. Lawrence, S. A. *Amines Synthesis, Properties and Applications;* Cambridge University Press: Cambridge, UK, 2006.
7. Pennington, L. D.; Collier, P. N.; Comer, E. *Med. Chem. Res.* **2023,** *32,* 1278–1293. doi:10.1007/s00044-023-03073-3
8. Heravi, M. M.; Zadsirjan, V. *RSC Adv.* **2020,** *10,* 44247–44311. doi:10.1039/d0ra09198g
9. Pennington, L. D.; Moustakas, D. T. *J. Med. Chem.* **2017,** *60,* 3552–3579. doi:10.1021/acs.jmedchem.6b01807
10. Vitaku, E.; Smith, D. T.; Njardarson, J. T. *J. Med. Chem.* **2014,** *57,* 10257–10274. doi:10.1021/jm501100b
11. Crisenza, G. E. M.; Melchiorre, P. *Nat. Commun.* **2020,** *11,* 803. doi:10.1038/s41467-019-13887-8
12. McAtee, R. C.; McClain, E. J.; Stephenson, C. R. J. *Trends Chem.* **2019,** *1,* 111–125. doi:10.1016/j.trechm.2019.01.008
13. Pitre, S. P.; Overman, L. E. *Chem. Rev.* **2022,** *122,* 1717–1751. doi:10.1021/acs.chemrev.1c00247
14. Choi, G. J.; Knowles, R. R. *J. Am. Chem. Soc.* **2015,** *137,* 9226–9229. doi:10.1021/jacs.5b05377
15. Miller, D. C.; Choi, G. J.; Orbe, H. S.; Knowles, R. R. *J. Am. Chem. Soc.* **2015,** *137,* 13492–13495. doi:10.1021/jacs.5b09671
16. Roos, C. B.; Demaerel, J.; Graff, D. E.; Knowles, R. R. *J. Am. Chem. Soc.* **2020,** *142,* 5974–5979. doi:10.1021/jacs.0c01332
17. Nguyen, L. Q.; Knowles, R. R. *ACS Catal.* **2016,** *6,* 2894–2903. doi:10.1021/acscatal.6b00486
18. Davies, J.; Svejstrup, T. D.; Fernandez Reina, D.; Sheikh, N. S.; Leonori, D. *J. Am. Chem. Soc.* **2016,** *138,* 8092–8095. doi:10.1021/jacs.6b04920
19. Ren, X.; Guo, Q.; Chen, J.; Xie, H.; Xu, Q.; Lu, Z. *Chem. – Eur. J.* **2016,** *22,* 18695–18699. doi:10.1002/chem.201603977
20. Galeotti, M.; Trasatti, C.; Sisti, S.; Salamone, M.; Bietti, M. *J. Org. Chem.* **2022,** *87,* 7456–7463. doi:10.1021/acs.joc.2c00955
21. Guo, W.; Wang, Q.; Zhu, J. *Chem. Soc. Rev.* **2021,** *50,* 7359–7377. doi:10.1039/d0cs00774a
22. Chu, J. C. K.; Rovis, T. *Nature* **2016,** *539,* 272–275. doi:10.1038/nature19810
23. Nguyen, T. M.; Nicewicz, D. A. *J. Am. Chem. Soc.* **2013,** *135,* 9588–9591. doi:10.1021/ja4031616
24. Nguyen, T. M.; Manohar, N.; Nicewicz, D. A. *Angew. Chem., Int. Ed.* **2014,** *53,* 6198–6201. doi:10.1002/anie.201402443
25. Gesmundo, N. J.; Grandjean, J.-M. M.; Nicewicz, D. A. *Org. Lett.* **2015,** *17,* 1316–1319. doi:10.1021/acs.orglett.5b00316
26. Roth, H. G.; Romero, N. A.; Nicewicz, D. A. *Synlett* **2016,** *27,* 714–723. doi:10.1055/s-0035-1561297

27. Xiong, L.; Tang, J. *Adv. Energy Mater.* **2021,** *11,* 2003216. doi:10.1002/aenm.202003216
28. Morse, P. D.; Nicewicz, D. A. *Chem. Sci.* **2015,** *6,* 270–274. doi:10.1039/c4sc02331e
29. Reed, N. L.; Lutovsky, G. A.; Yoon, T. P. *J. Am. Chem. Soc.* **2021,** *143,* 6065–6070. doi:10.1021/jacs.1c02747
30. Tlili, A.; Lakhdar, S. *Angew. Chem., Int. Ed.* **2021,** *60,* 19526–19549. doi:10.1002/anie.202102262
31. Joshi-Pangu, A.; Lévesque, F.; Roth, H. G.; Oliver, S. F.; Campeau, L.-C.; Nicewicz, D.; DiRocco, D. A. *J. Org. Chem.* **2016,** *81,* 7244–7249. doi:10.1021/acs.joc.6b01240
32. Ohkubo, K.; Matsumoto, S.; Asahara, H.; Fukuzumi, S. *ACS Catal.* **2024,** *14,* 2671–2684. doi:10.1021/acscatal.3c06111
33. López-Agudelo, V. A.; Gómez-Ríos, D.; Ramirez-Malule, H. *Antibiotics (Basel, Switz.)* **2021,** *10,* 84. doi:10.3390/antibiotics10010084
34. Saudagar, P. S.; Survase, S. A.; Singhal, R. S. *Biotechnol. Adv.* **2008,** *26,* 335–351. doi:10.1016/j.biotechadv.2008.03.002
35. Brown, A. G.; Butterworth, D.; Cole, M.; Hanscomb, G.; Hood, J. D.; Reading, C.; Rolinson, G. N. *J. Antibiot.* **1976,** *29,* 668–669. doi:10.7164/antibiotics.29.668
36. Brown, A. G.; Corbett, D. F.; Goodacre, J.; Harbridge, J. B.; Howarth, T. T.; Ponsford, R. J.; Stirling, I.; King, T. J. *J. Chem. Soc., Perkin Trans. 1* **1984,** 635–650. doi:10.1039/p19840000635
37. Brown, D.; Evans, J. R.; Fletton, R. A. *J. Chem. Soc., Chem. Commun.* **1979,** 282–283. doi:10.1039/c39790000282
38. Wanning, M.; Zähner, H.; Krone, B.; Zeeck, A. *Tetrahedron Lett.* **1981,** *22,* 2539–2540. doi:10.1016/s0040-4039(01)90514-3
39. Pruess, D. L.; Kellett, M. *J. Antibiot.* **1983,** *36,* 208–212. doi:10.7164/antibiotics.36.208
40. Evans, R. H., Jr.; Ax, H.; Jacoby, A.; Williams, T. H.; Jenkins, E.; Scannell, J. P. *J. Antibiot.* **1983,** *36,* 213–216. doi:10.7164/antibiotics.36.213
41. King, H. D.; Langhärig, J.; Sanglier, J. J. *J. Antibiot.* **1986,** *39,* 510–515. doi:10.7164/antibiotics.39.510
42. Naegeli, H. V.; Loosli, H.-R.; Nussbaumer, A. *J. Antibiot.* **1986,** *39,* 516–524. doi:10.7164/antibiotics.39.516
43. Hoppe, D.; Hilpert, T. *Tetrahedron* **1987,** *43,* 2467–2474. doi:10.1016/s0040-4020(01)81652-5
44. Bachi, M. D.; Frolow, F.; Hoornaert, C. *J. Org. Chem.* **1983,** *48,* 1841–1849. doi:10.1021/jo00159a010
45. Barrett, A. G. M.; Baugh, S. P. D.; Gibson, V. C.; Giles, M. R.; Marshall, E. L.; Procopiou, P. A. *Chem. Commun.* **1997,** 155–156. doi:10.1039/a607308e
46. Staszewska-Krajewska, O.; Bocian, W.; Maciejko, M.; Szcześniak, P.; Szymczak, K.; Chmielewski, M.; Furman, B. *ARKIVOC* **2014,** No. iii, 143–153. doi:10.3998/ark.5550190.p008.450
47. Bryden, M. A.; Zysman-Colman, E. *Chem. Soc. Rev.* **2021,** *50,* 7587–7680. doi:10.1039/d1cs00198a
48. Speckmeier, E.; Fischer, T. G.; Zeitler, K. *J. Am. Chem. Soc.* **2018,** *140,* 15353–15365. doi:10.1021/jacs.8b08933
49. Schepp, N. P.; Johnston, L. J. *J. Am. Chem. Soc.* **1996,** *118,* 2872–2881. doi:10.1021/ja9535468
50. Allin, S. M.; James, S. L.; Martin, W. P.; Smith, T. A. D. *Tetrahedron Lett.* **2001,** *42,* 3943–3946. doi:10.1016/s0040-4039(01)00613-x
51. Allin, S. M.; James, S. L.; Martin, W. P.; Smith, T. A. D.; Elsegood, M. R. J. *J. Chem. Soc., Perkin Trans. 1* **2001,** 3029–3036. doi:10.1039/b105402n
52. Brasholz, M. Acridinium Dyes and Quinones in Photocatalysis. In *Photocatalysis in Organic Synthesis;* König, B., Ed.; Science of Synthesis, Vol. 2018/6; Thieme: Stuttgart, Germany, 2018; pp 371–390. doi:10.1055/sos-sd-229-00224
53. Fukuzumi, S.; Ohkubo, K.; Suenobu, T. *Acc. Chem. Res.* **2014,** *47,* 1455–1464. doi:10.1021/ar400200u
54. Tsudaka, T.; Kotani, H.; Ohkubo, K.; Nakagawa, T.; Tkachenko, N. V.; Lemmetyinen, H.; Fukuzumi, S. *Chem. – Eur. J.* **2017,** *23,* 1306–1317. doi:10.1002/chem.201604527
55. Zilate, B.; Fischer, C.; Sparr, C. *Chem. Commun.* **2020,** *56,* 1767–1775. doi:10.1039/c9cc08524f
56. White, A. R.; Wang, L.; Nicewicz, D. A. *Synlett* **2019,** *30,* 827–832. doi:10.1055/s-0037-1611744
57. Glover, S. A.; Rosser, A. A. *J. Org. Chem.* **2012,** *77,* 5492–5502. doi:10.1021/jo300347k
58. Mucsi, Z.; Tsai, A.; Szori, M.; Chass, G. A.; Viskolcz, B.; Csizmadia, I. G. *J. Phys. Chem. A* **2007,** *111,* 13245–13254. doi:10.1021/jp0759325
59. Didier, D.; Baumann, A. N.; Eisold, M. *Tetrahedron Lett.* **2018,** *59,* 3975–3987. doi:10.1016/j.tetlet.2018.09.055
60. Fukuzumi, S.; Kotani, H.; Ohkubo, K.; Ogo, S.; Tkachenko, N. V.; Lemmetyinen, H. *J. Am. Chem. Soc.* **2004,** *126,* 1600–1601. doi:10.1021/ja038656q
61. Ohkubo, K.; Mizushima, K.; Iwata, R.; Souma, K.; Suzuki, N.; Fukuzumi, S. *Chem. Commun.* **2010,** *46,* 601–603. doi:10.1039/b920606j

License and Terms

BEILSTEIN JOURNAL OF ORGANIC CHEMISTRY

Giese-type alkylation of dehydroalanine derivatives via silane-mediated alkyl bromide activation

Perry van der Heide‡[1,2], Michele Retini‡[3], Fabiola Fanini[3], Giovanni Piersanti[3], Francesco Secci[1], Daniele Mazzarella[4,5], Timothy Noël[2] and Alberto Luridiana*[1]

Letter

Open Access

Address:
[1]Department of Chemical and Geological Sciences, University of Cagliari, S.S. 554, bivio per Sestu, 09042 Monserrato (CA), Italy, [2]Flow Chemistry Group, Van 't Hoff Institute for Molecular Sciences (HIMS), University of Amsterdam Science Park 904, 1098 XH Amsterdam, The Netherlands, [3]Department of Biomolecular Sciences, University of Urbino "Carlo Bo", Piazza Rinascimento 6, 61029 Urbino, Italy, [4]Department of Chemical Sciences and Technologies, University of Rome "Tor Vergata" Via della Ricerca Scientifica, 1, 00133 Rome, Italy, and [5]Department of Chemical Sciences, University of Padova Institution, Via Francesco Marzolo, 1, 35131 Padova, Italy

Email:
Alberto Luridiana* - alberto.luridiana@unica.it

* Corresponding author ‡ Equal contributors

Keywords:
dehydroalanine; Giese-type reaction; hydroalkylation; photocatalysis; water

Beilstein J. Org. Chem. **2024,** *20,* 3274–3280.
https://doi.org/10.3762/bjoc.20.271

Received: 09 October 2024
Accepted: 26 November 2024
Published: 17 December 2024

This article is part of the thematic issue "Photocatalysis and photochemistry in organic synthesis".

Associate Editor: C. Stephenson

Abstract

The rising popularity of bioconjugate therapeutics has led to growing interest in late-stage functionalization (LSF) of peptide scaffolds. α,β-Unsaturated amino acids like dehydroalanine (Dha) derivatives have emerged as particularly useful structures, as the electron-deficient olefin moiety can engage in late-stage functionalization reactions, like a Giese-type reaction. Cheap and widely available building blocks like organohalides can be converted into alkyl radicals by means of photoinduced silane-mediated halogen-atom transfer (XAT) to offer a mild and straightforward methodology of alkylation. In this research, we present a metal-free strategy for the photochemical alkylation of dehydroalanine derivatives. Upon abstraction of a hydride from tris(trimethylsilyl)silane (TTMS) by an excited benzophenone derivative, the formed silane radical can undergo a XAT with an alkyl bromide to generate an alkyl radical. Consequently, the alkyl radical undergoes a Giese-type reaction with the Dha derivative, forming a new $C(sp^3)$–$C(sp^3)$ bond. The reaction can be performed in a phosphate-buffered saline (PBS) solution and shows post-functionalization prospects through pathways involving classical peptide chemistry.

Introduction

The construction of $C(sp^3)$–$C(sp^3)$ bonds is a highly important target in synthetic organic chemistry. Historically, polar conjugate additions have been a benchmark method for constructing these bonds by functionalizing an electron-deficient olefin [1-3]. Recently, however, radical-based approaches have also gained widespread attention for their unique advantages in these

transformations [4]. Radical chemistry often exhibits complementary reactivity to two-electron pathways and can be performed with high selectivity, atom economy, and functional group tolerance [5]. A well-known radical pathway for the functionalization of an electron-deficient olefin is the Giese reaction (Figure 1) [6,7]. This reaction involves the hydroalkylation of the olefin via radical addition (RA), followed by either hydrogen-atom transfer (HAT) or single-electron transfer (SET) and protonation.

Traditionally, alkyl radicals have been produced from alkyl halides, using azobisisobutyronitrile (AIBN) as initiator, promoting a tin-mediated XAT (Figure 1a) [8,9]. However, tin-based compounds are highly toxic and require harsh conditions for the initiation event.

Fortunately, a renaissance in the field of photochemistry has introduced new ways of generating radicals like photoredox catalysis and via electron donor–acceptor (EDA) complexes [10-13]. These advances, coupled with modern electrochemical methods, chemical reactor engineering and light emitting diodes (LED), have eliminated the need for thermal radical activation, resulting in milder and safer reaction conditions [14-16]. Given the toxicity of tin-based compounds, there has been significant interest in developing alternative halogen-atom-transfer reagents. Borane, alkylamine, and silane compounds have emerged as effective XAT reagents upon photocatalytic activation (Figure 1b) [17-21]. A photocatalytic HAT or SET generates the corresponding boryl, α-amino or silyl radical, which can abstract a halogen atom from alkyl halides to form the corresponding alkyl radical.

However, the use of TTMS as a XAT reagent had already been established by Chatgilialoglu et al. [22] under non-photoredox conditions, MacMillan et al. [23] sparked renewed interest in silanes as XAT reagents by generating a tris(trimethylsilyl)silyl radical through photoredox catalysis for arylation reactions [22,23]. In 2018, Balsells et al. [24] reported a similar strategy to generate alkyl radicals and explored the feasibility of a Giese-type reaction (Figure 1c). More recently, Gaunt et al. [25] showed that irradiation of alkyl iodides combined with TTMS leads to the formation of an alkyl radical, which can be used in a Giese-type reaction without the need of a photocatalyst (Figure 1d) [25]. Noël et al. [26] have further extended this approach to include alkyl bromides (Figure 1e) [26]. Despite the effectiveness of the photolysis, benzophenone derivatives have also been shown to enhance the productivity of silane-mediated conjugate additions, using alkyl halides [27].

Amid the growing popularity of biomolecular drug candidates, the late-stage modification of peptide scaffolds has gained significant importance [28]. A particularly interesting class of amino acids for late-stage diversification consists of dehydroamino acids (Dha). Dha derivatives have shown modifica-

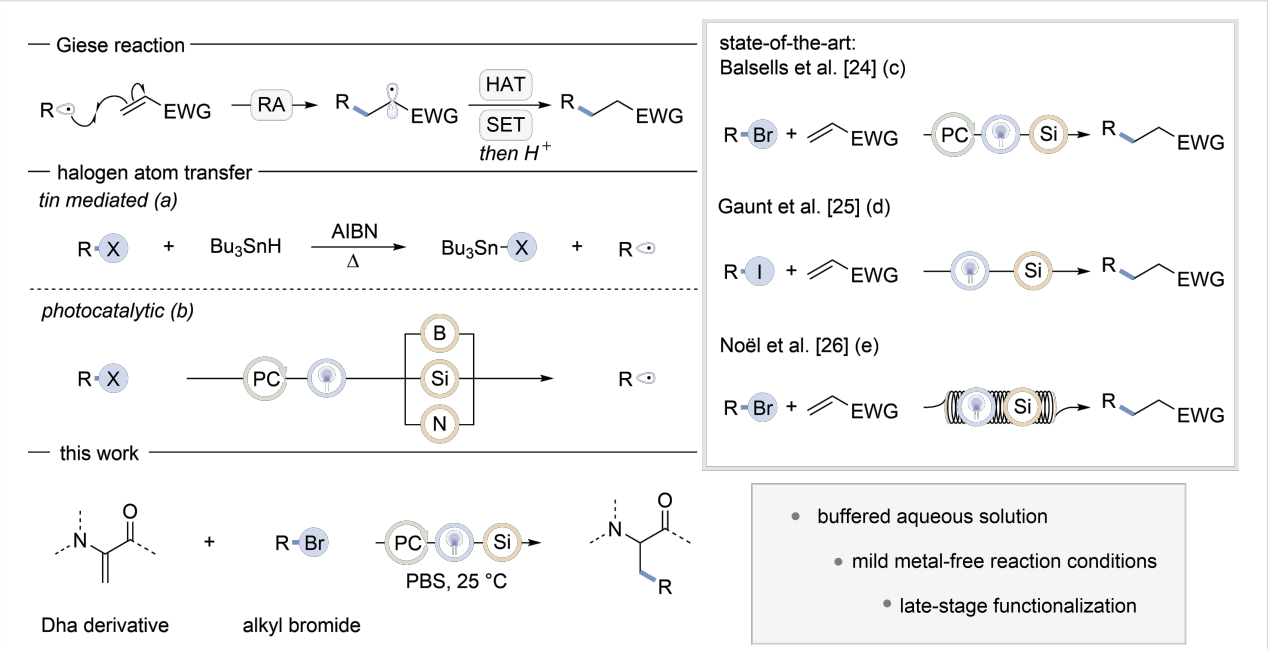

Figure 1: Giese reaction: Radical addition on olefins with an electron-withdrawing group (EWG) followed by a HAT or SET and protonation; halogen-atom transfer: (a) tin-mediated XAT, (b) XAT initiated by a photocatalyst (PC) and mediated by boranes (B), silanes (Si) or alkylamines (N); state-of-the-art: (c) silane-mediated alkylation initiated by a photocatalyst, (d) silane-mediated alkylation initiated by photolysis of alkyl iodides, (e) silane-mediated alkylation initiated by photolysis of alkyl bromides in flow; this work: silane-mediated alkylation of Dha derivatives initiated by a photocatalyst.

tion potential by means of polar, metal-, or organo-catalyzed and radical additions [29-36]. As such, Dha derivatives make an excellent candidate for exploring a photochemical Giese-type reaction [37]. To foster a physiological reaction environment, reactions can be conducted in aqueous solution, meeting important requirements with regard to bioorthogonal chemistry [38].

Considering previous research that demonstrated photochemical hydrogen atom abstraction by benzophenone derivatives from trialkylsilyl hydrides [27], as well as advances in alkyl radical formation using these hydrides, we sought to combine these findings. Herein, we report a photochemical alkylation methodology targeting the olefin moiety of Dha derivatives, conducted in an aqueous solution for the aforementioned bioorthogonal advantages.

Results and Discussion

Inspired by previously conducted research concerning benzophenone hydrogen-atom transfer and silane-mediated activation of alkyl bromides to perform a photochemical Giese reaction, methyl 2-(1,3-dioxoisoindolin-2-yl)acrylate (**1**) and bromocyclohexane (**2**) were dissolved in CH_3CN (0.1 M) together with a stoichiometric amount of tris(trimethylsilyl)silane and a substoichiometric amount of (4-methoxyphenyl)(4-(trifluoromethyl)phenyl)methanone (BP **I**) (Table 1) [26,27].

The reaction was performed in batch, using a 390 nm Kessil UV-A lamp, stirring at 600 rpm overnight at 25 °C (see Supporting Information File 1 for a more detailed optimization).

The initial reaction, using CH_3CN as solvent, led to formation of methyl 3-cyclohexyl-2-(1,3-dioxoisoindolin-2-yl)propanoate (**3**, 51% yield, 85% conv.; Table 1, entry 1). To demonstrate the importance of the photocatalyst, BP **I** was excluded (Table 1, entry 2), resulting in a slightly higher conversion and a decrease in product formation (38% yield, 90% conv.), meaning BP **I** increases the productivity of the reaction. Having established that the reaction works in CH_3CN, we evaluated its compatibility with water. To our delight, the reaction in water provided full conversion and a higher yield than the one observed in CH_3CN (58% yield, 100% conv.; Table 1, entry 3). These conditions were further refined by adding of phosphate-buffered saline and decreasing the amount of $(TMS)_3SiH$ to 1.1 equiv, as no further increase in yield was noticed during the optimization. Similar to the reaction in deionized water, all entries with PBS solution reached a full conversion. While the yield of the reaction with a 0.1 M PBS solution was slightly lower than that of the reaction in deionized water (44% yield, 100% conv.; Table 1, entry 4), a 0.2 M PBS solution resulted in an increased yield (60% yield, 100% conv.; Table 1, entry 5). Upon increasing the concentration of the PBS solution to 0.4 M,

Table 1: Methyl 2-(1,3-dioxoisoindolin-2-yl)acrylate (**1**, 0.5 mmol), bromocyclohexane (**2**, 1.25 mmol), tris(trimethylsilyl)silane (0.55 mmol), (4-methoxyphenyl)(4-(trifluoromethyl)phenyl)methanone (0.1 mmol), PBS 0.2 M solution (2.5 mL), λ = 390 nm, 25 °C, overnight. The yield of **3** was calculated by ^1H NMR with 1,1,2-trichloroethene as external standard.

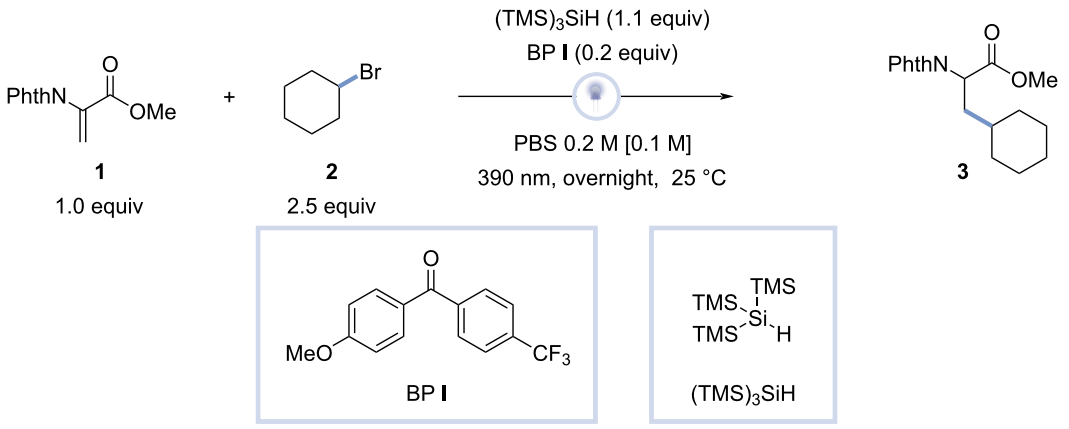

Entry	Deviation from the reaction conditions	Conversion **1** (%)	NMR yield **3** (%)
1	CH_3CN instead of PBS 0.2 M; 1.5 equiv $(TMS)_3SiH$	85	51
2	CH_3CN instead of PBS 0.2 M; no BP **I**; 1.5 equiv $(TMS)_3SiH$	90	38
3	H_2O instead of PBS 0.2 M; 1.5 equiv $(TMS)_3SiH$	100	58
4	PBS 0.1 M instead of PBS 0.2 M	100	44
5	none	100	60
6	PBS 0.4 M instead of PBS 0.2 M	100	60
7	**3 hours**	**100**	**67**

no change in yield was observed (60% yield, 100% conv.; Table 1, entry 6). Lastly, the optimal reaction time was determined to be 3 hours (67% yield, 100% conv.; Table 1, entry 7). Having optimized the reaction conditions, a scope of primary, secondary, and tertiary alkyl bromides and different Dha derivatives was investigated (Figure 2).

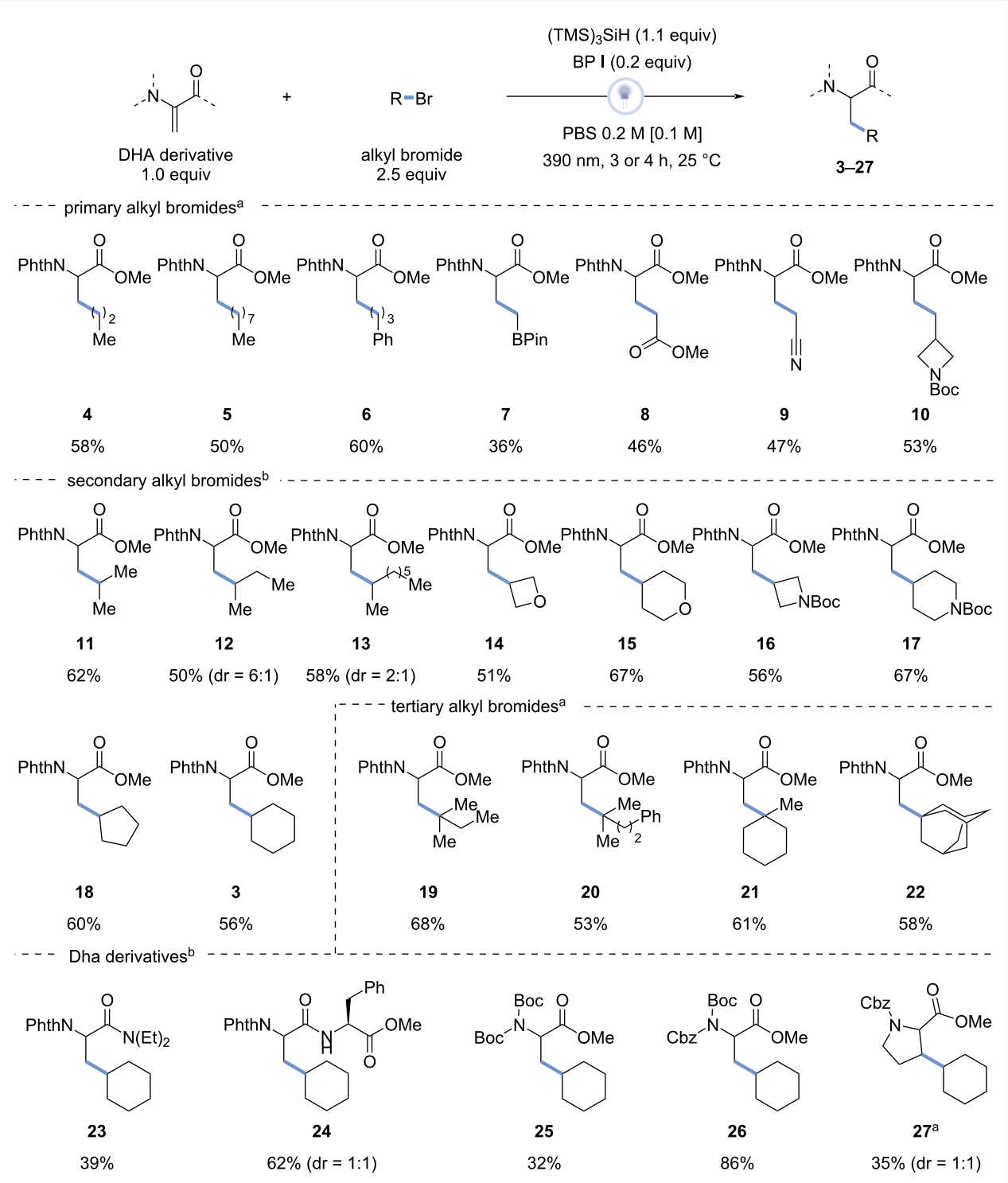

Figure 2: Alkyl bromide and Dha derivative scope. Reaction conditions: Dha derivative (0.5 mmol), alkyl bromide (1.25 mmol), tris(trimethylsilyl)silane (0.55 mmol), (4-methoxyphenyl)(4-(trifluoromethyl)phenyl)methanone (0.1 mmol), PBS 0.2 M solution (2.5 mL), λ = 390 nm, 25 °C. [a]4 hours of reaction time, [b]3 hours of reaction time. The isolated product yields are reported.

A slight modification of the reaction protocol was used in regard to primary and tertiary alkyl bromides, requiring a longer reaction time (4 hours instead of 3 hours) to achieve full conversion.

The reaction worked well with aliphatic primary bromides (**4**–**10**). However, a longer chain length slightly decreased the yield, comparing compound **4** (58%) to compound **5** (50%). The reaction was not influenced by the presence of phenyl rings, as the yield of compound **6** (60%) was comparable to the yield of **4**. Besides, the introduction of a boronic pinacol ester group, useful for subsequent post-functionalization, compound **7** was achieved in a relatively lower yield of 36%. Interestingly, the reaction also worked adequately for primary alkyl bromides with electron-withdrawing groups as demonstrated in compounds **8** (46%) and **9** (47%). Moreover, primary alkyl bromides like bromomethylazetidines as used in compound **10** (53%) also resulted in decent yields. Acyclic secondary alkyl substrates all resulted in good yields (**11**–**13**, 50–62%). For the secondary alkyl substrates, a higher yield was notably obtained for compound **13** with a longer chain length than for **12**. Similarly, the secondary cyclic alkyl substrates used in compound **18** (60%) and **3** (56%) worked well for this reaction. Besides, oxygen-containing compounds **14** and **15** were obtained in yields of 51% and 67% and medicinally interesting groups like the azetidine in compound **16** (56%) and the piperidine in compound **17** (67%) also resulted in good yields. Concerning tertiary alkyl substrates, acyclic alkyl substrates used in compound **19** (68%) and **20** (53%) as well as cyclic alkyl substrates like bromomethylcyclohexane used in compound **21** (61%) and bromoadamantane in compound **22** (58%) were obtained in satisfactory yields.

Subsequently, different Dha derivatives were subjected to the optimized reaction conditions, using bromocyclohexane (**2**) as the alkyl bromide. In order to explore the effect of the presence of an amide moiety in the Dha derivatives, a tertiary amide was firstly used to exclude selectivity issues arising from the hydrogen atoms of the amide functionality, yielding compound **23** in synthetically useful yield (39%). Interestingly, a secondary amide was formed in a higher yield of compound **24** (62%) compared to a Dha with a tertiary amide on the same position. Alternatively, the use of a double Boc-protected Dha resulted in a rather low yield of compound **25** (32%), while varying one Boc-protecting group with a Cbz-protecting group increased the yield substantially to 86% for compound **26**. In addition, the use of a cyclic, *N*-Cbz-protected Michael acceptor, derived from proline, allowed for preparation of compound **27** with a 35% yield in 4 hours without control of diastereoselectivity (dr = 1:1).

Finally, to prove that the optimized reaction also works at a larger scale, the model reaction was carried out on a 2.2 mmol scale (Figure 3), obtaining a slightly elevated yield (67%) compared to compound **3**, which was previously formed at a 0.5 mmol scale.

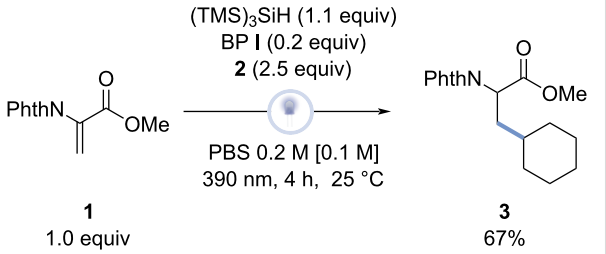

Figure 3: Scaled-up reaction. Reaction conditions: Dha derivative (2.2 mmol), alkyl bromide (5.4 mmol), tris(trimethylsilyl)silane (2.4 mmol), (4-methoxyphenyl)(4-(trifluoromethyl)phenyl)methanone (0.4 mmol), PBS 0.2 M solution (10.8 mL), λ = 390 nm, 25 °C, 4 hours, isolated product yield.

Conclusion

In conclusion, a photochemical methodology to promote the metal-free alkylation of dehydroalanine derivatives was developed, by means of silane-mediated alkyl bromide activation. The biocompatibility of the reaction enabled by the PBS solution and the mild photochemical reaction conditions makes the transformation useful for late-stage functionalization under physiological conditions. Besides, the reaction was successfully scaled up by roughly four times, leading to a slight increase in chemical yield.

Supporting Information

Supporting Information File 1

^{1}H NMR, ^{13}C NMR, and HRMS spectra of all the synthesized compounds.
[https://www.beilstein-journals.org/bjoc/content/supplementary/1860-5397-20-271-S1.pdf]

Acknowledgements

We are grateful to University Research Services Center (CeSAR)-UniCA for the analysis service.

Funding

P. H. thanks the Erasmus+ traineeship program. The research contract (63-G-19602-1) of M.R. is co-financed by the European Union "FSE-REACT-EU, PON Research and innovation 2014-2020 DM 1062/2021" (CUP H31B21009610007). A.L.

thanks the MUR for a Young Researchers Seal of Excellence fellowship (PlaDisPho) SOE_0000091 (PNRR).

ORCID® iDs

Perry van der Heide - https://orcid.org/0009-0006-3138-4379
Michele Retini - https://orcid.org/0000-0003-0218-8505
Giovanni Piersanti - https://orcid.org/0000-0003-0418-7143
Francesco Secci - https://orcid.org/0000-0003-0443-2890
Alberto Luridiana - https://orcid.org/0000-0002-7828-9866

Data Availability Statement

All data that supports the findings of this study is available in the published article and/or the supporting information of this article.

References

1. Yang, L.; Huang, H. *Chem. Rev.* **2015,** *115,* 3468–3517. doi:10.1021/cr500610p
2. Csákÿ, A. G.; de La Herrán, G.; Murcia, M. C. *Chem. Soc. Rev.* **2010,** *39,* 4080–4102. doi:10.1039/b924486g
3. Ballini, R.; Bosica, G.; Fiorini, D.; Palmieri, A.; Petrini, M. *Chem. Rev.* **2005,** *105,* 933–972. doi:10.1021/cr040602r
4. Renaud, P.; Sibi, M. P., Eds. *Radicals in Organic Synthesis;* Wiley-VCH: Weinheim, Germany, 2001. doi:10.1002/9783527618293
5. Castellino, N. J.; Montgomery, A. P.; Danon, J. J.; Kassiou, M. *Chem. Rev.* **2023,** *123,* 8127–8153. doi:10.1021/acs.chemrev.2c00797
6. Giese, B.; Meister, J. *Angew. Chem., Int. Ed. Engl.* **1977,** *16,* 178–179. doi:10.1002/anie.197701781
7. Kitcatt, D. M.; Nicolle, S.; Lee, A.-L. *Chem. Soc. Rev.* **2022,** *51,* 1415–1453. doi:10.1039/d1cs01168e
8. Kuivila, H. G.; Menapace, L. W. *J. Org. Chem.* **1963,** *28,* 2165–2167. doi:10.1021/jo01044a001
9. Giese, B.; Dupuis, J. *Angew. Chem., Int. Ed. Engl.* **1983,** *22,* 622–623. doi:10.1002/anie.198306221
10. Shaw, M. H.; Twilton, J.; MacMillan, D. W. C. *J. Org. Chem.* **2016,** *81,* 6898–6926. doi:10.1021/acs.joc.6b01449
11. Crisenza, G. E. M.; Mazzarella, D.; Melchiorre, P. *J. Am. Chem. Soc.* **2020,** *142,* 5461–5476. doi:10.1021/jacs.0c01416
12. McClain, E. J.; Monos, T. M.; Mori, M.; Beatty, J. W.; Stephenson, C. R. J. *ACS Catal.* **2020,** *10,* 12636–12641. doi:10.1021/acscatal.0c03837
13. Wortman, A. K.; Stephenson, C. R. J. *Chem* **2023,** *9,* 2390–2415. doi:10.1016/j.chempr.2023.06.013
14. Yuan, Y.; Yang, J.; Lei, A. *Chem. Soc. Rev.* **2021,** *50,* 10058–10086. doi:10.1039/d1cs00150g
15. Buglioni, L.; Raymenants, F.; Slattery, A.; Zondag, S. D. A.; Noël, T. *Chem. Rev.* **2022,** *122,* 2752–2906. doi:10.1021/acs.chemrev.1c00332
16. Wan, T.; Wen, Z.; Laudadio, G.; Capaldo, L.; Lammers, R.; Rincón, J. A.; García-Losada, P.; Mateos, C.; Frederick, M. O.; Broersma, R.; Noël, T. *ACS Cent. Sci.* **2022,** *8,* 51–56. doi:10.1021/acscentsci.1c01109
17. Chatgilialoglu, C.; Ferreri, C.; Landais, Y.; Timokhin, V. I. *Chem. Rev.* **2018,** *118,* 6516–6572. doi:10.1021/acs.chemrev.8b00109
18. Zhang, Z.; Tilby, M. J.; Leonori, D. *Nat. Synth.* **2024,** *3,* 1221–1230. doi:10.1038/s44160-024-00587-5
19. Constantin, T.; Zanini, M.; Regni, A.; Sheikh, N. S.; Juliá, F.; Leonori, D. *Science* **2020,** *367,* 1021–1026. doi:10.1126/science.aba2419
20. Wan, T.; Capaldo, L.; Ravelli, D.; Vitullo, W.; de Zwart, F. J.; de Bruin, B.; Noël, T. *J. Am. Chem. Soc.* **2023,** *145,* 991–999. doi:10.1021/jacs.2c10444
21. Poletti, L.; Massi, A.; Ragno, D.; Droghetti, F.; Natali, M.; De Risi, C.; Bortolini, O.; Di Carmine, G. *Org. Lett.* **2023,** *25,* 4862–4867. doi:10.1021/acs.orglett.3c01660
22. Chatgilialoglu, C.; Griller, D.; Lesage, M. *J. Org. Chem.* **1988,** *53,* 3641–3642. doi:10.1021/jo00250a051
23. Zhang, P.; Le, C. C.; MacMillan, D. W. C. *J. Am. Chem. Soc.* **2016,** *138,* 8084–8087. doi:10.1021/jacs.6b04818
24. ElMarrouni, A.; Ritts, C. B.; Balsells, J. *Chem. Sci.* **2018,** *9,* 6639–6646. doi:10.1039/c8sc02253d
25. Mistry, S.; Kumar, R.; Lister, A.; Gaunt, M. J. *Chem. Sci.* **2022,** *13,* 13241–13247. doi:10.1039/d2sc03516b
26. Fanini, F.; Luridiana, A.; Mazzarella, D.; Alfano, A. I.; van der Heide, P.; Rincón, J. A.; García-Losada, P.; Mateos, C.; Frederick, M. O.; Nuño, M.; Noël, T. *Tetrahedron Lett.* **2023,** *117,* 154380. doi:10.1016/j.tetlet.2023.154380
27. Luridiana, A.; Mazzarella, D.; Capaldo, L.; Rincón, J. A.; García-Losada, P.; Mateos, C.; Frederick, M. O.; Nuño, M.; Jan Buma, W.; Noël, T. *ACS Catal.* **2022,** *12,* 11216–11225. doi:10.1021/acscatal.2c03805
28. Wang, L.; Wang, N.; Zhang, W.; Cheng, X.; Yan, Z.; Shao, G.; Wang, X.; Wang, R.; Fu, C. *Signal Transduction Targeted Ther.* **2022,** *7,* 48. doi:10.1038/s41392-022-00904-4
29. Bogart, J. W.; Bowers, A. A. *Org. Biomol. Chem.* **2019,** *17,* 3653–3669. doi:10.1039/c8ob03155j
30. Jousseaume, T.; Wurz, N. E.; Glorius, F. *Angew. Chem., Int. Ed.* **2011,** *50,* 1410–1414. doi:10.1002/anie.201006548
31. Key, H. M.; Miller, S. J. *J. Am. Chem. Soc.* **2017,** *139,* 15460–15466. doi:10.1021/jacs.7b08775
32. Retini, M.; Bartolucci, S.; Bartoccini, F.; Piersanti, G. *Chem. – Eur. J.* **2022,** *28,* e202201994. doi:10.1002/chem.202201994
33. Kaplaneris, N.; Akdeniz, M.; Fillols, M.; Arrighi, F.; Raymenants, F.; Sanil, G.; Gryko, D. T.; Noël, T. *Angew. Chem., Int. Ed.* **2024,** *63,* e202403271. doi:10.1002/anie.202403271
34. Aycock, R. A.; Pratt, C. J.; Jui, N. T. *ACS Catal.* **2018,** *8,* 9115–9119. doi:10.1021/acscatal.8b03031
35. Sim, J.; Campbell, M. W.; Molander, G. A. *ACS Catal.* **2019,** *9,* 1558–1563. doi:10.1021/acscatal.8b04284
36. Gu, X.; Zhang, Y.-A.; Zhang, S.; Wang, L.; Ye, X.; Occhialini, G.; Barbour, J.; Pentelute, B. L.; Wendlandt, A. E. *Nature* **2024,** *634,* 352–358. doi:10.1038/s41586-024-07988-8
37. Peng, X.; Xu, K.; Zhang, Q.; Liu, L.; Tan, J. *Trends Chem.* **2022,** *4,* 643–657. doi:10.1016/j.trechm.2022.04.008
38. Lim, R. K. V.; Lin, Q. *Chem. Commun.* **2010,** *46,* 1589. doi:10.1039/b925931g

License and Terms